

# NATIONAL ADVISORY COMMITTEE FOR AERONAUTICS

TECHNICAL NOTE 1925

## LINE-VORTEX THEORY FOR CALCULATION OF SUPERSONIC DOWNWASH

By Harold Mirels and Rudolph C. Haefeli

Lewis Flight Propulsion Laboratory  
Cleveland, Ohio

**DISTRIBUTION STATEMENT A**  
Approved for Public Release  
Distribution Unlimited



Washington  
August 1949

Reproduced From  
Best Available Copy

20000001  
311

PTIC QUALITY INSPECTED 4

AQM-00-10-334

NATIONAL ADVISORY COMMITTEE FOR AERONAUTICS

TECHNICAL NOTE 1925

LINE-VORTEX THEORY FOR CALCULATION OF  
SUPersonic DOWNWASH

By Harold Mirels and Rudolph C. Haefeli

SUMMARY

The perturbation field induced by a line vortex in a supersonic stream and the downwash behind a supersonic lifting surface are examined for the purpose of establishing approximate methods for determining the downwash behind supersonic wings.

Lifting-line methods are presented for calculating supersonic downwash. An unbent lifting line (horseshoe-vortex system) is used to compute the downwash behind rectangular and triangular wings and the results are compared with the exact linearized solutions. The chordwise position of the lifting line giving the best average agreement with the exact solution is noted for each wing. A bent lifting line is used to approximate the triangular wing, and the results are in good agreement with the exact solution except for points within  $1/2$  chord of the wing trailing edge. The use of a bent lifting line seems promising for obtaining accurate estimates of the downwash behind swept wings.

INTRODUCTION

Several methods for obtaining the downwash behind supersonic wings based on linearized theory have been presented. These methods utilize conical superposition (reference 1), doublet distributions (references 2 and 3), or vortex distributions (references 4 and 5). Each of these methods has certain disadvantages. Conical superposition is restricted to wings having plan forms composed of straight-line segments and is cumbersome for other than trapezoidal or triangular plan forms. The doublet and vortex distributions apply to arbitrary plan forms, but provide integral expressions for downwash that are generally very tedious to evaluate. The complexity of these expressions indicates that there is a need for a straight-forward procedure for obtaining reasonably accurate, if not exact, downwash solutions.

A logical approach to the development of a simplified super-sonic downwash theory is to derive the supersonic analogues of the line-vortex procedures that have proved valuable in subsonic theory. Certain differences exist, however, between the properties of vortices in a supersonic stream and vortices in a subsonic stream. Similarly, the downwash fields behind subsonic and supersonic wings differ in certain respects. These differences must be investigated before an extension of subsonic techniques is possible.

The present report, prepared at the NACA Lewis laboratory, has three main objectives: (1) The downwash field induced by a super-sonic line vortex of constant slope is derived and discussed; (2) the downwash behind a supersonic lifting surface is examined and related to the downwash field induced by line vortices; and (3) lifting-line methods for computing downwash are presented and calculations based on these methods are compared with the exact linearized solutions. Zero-thickness wings (lifting surfaces) are considered throughout.

#### SYMBOLS

The following symbols are used throughout this report:

$x, x_1$	Cartesian coordinate system
$y, y_1$	
$z, z_1$	
$u$	
$v$	perturbation velocities
$w$	
$\bar{i}$	
$\bar{j}$	unit vectors
$\bar{k}$	
$\xi$	
$\eta$	components of vortex vector (three-dimensional field)
$\zeta$	

$\xi'$   
 $\eta'$   
 $\zeta'$  } components of vortex vector (vortex sheet)

b wing span

C function used in evaluation of finite part of divergent integral (equation (7))

$c_p$  local wing pressure coefficient

$c_e$  effective chord of bent lifting line

$c_r$  root chord of wing

E complete elliptic integral of second kind with modulus

$$\sqrt{1 - \left(\frac{b}{2c_r}\right)^2}$$

$$G_1(m) = \frac{(Y_1 - m_1 X_1)(\beta^2 m_1 Y_1 - X_1)}{r_1 [(Y_1 - m_1 X_1)^2 + (1 - \beta^2 m_1^2) Z_1^2]}$$

$$G_1(0) = \frac{-1}{r_1} \frac{X_1 Y_1}{(Y_1^2 + Z_1^2)}$$

L(y) spanwise lift distribution

M free-stream Mach number

m slope of line vortex or lifting line

$$r_1 = \sqrt{X_1^2 - \beta^2 Y_1^2 - \beta^2 Z_1^2}$$

U free-stream velocity (taken in x-direction)

$$X_1 = x - x_1$$

$$Y_1 = y - y_1$$

$$Z_1 = z - z_1$$

$\alpha$  angle of attack  
 $\beta$  cotangent of Mach angle  $\sqrt{M^2 - 1}$   
 $\epsilon$  integration interval  
 $\kappa$  circulation  
 $\varphi$  perturbation-velocity potential  
 $\Delta\varphi$   $\varphi_T - \varphi_B$   
 $\rho$  free-stream density  
 $\sigma$  cross-sectional area of vortex tube  
 $\Gamma$  spanwise distribution of wing circulation  
 $\Gamma_m$  wing circulation at midspan  
 $\omega$  resultant vorticity  $(\xi^2 + \eta^2 + \zeta^2)^{1/2}$   
 $\int$  finite part of divergent integral  
 $\oint$  line integral along closed curve

Subscripts:

$a, b$  points of intersection of forward Mach cone with line vortex, lifting line, or edge of vortex sheet  
 $B$  bottom surface of  $z = 0$  plane  
 $C$  line integration  
 $i = 1, 2, 3, \dots, n$  points on vortex lines  
 $l$  plan-form leading edge  
 $S$  surface integration  
 $T$  top surface of  $z = 0$  plane  
 $t$  plan-form trailing edge  
 $V$  volume integration  
 $\circ$  variable of integration

## Superscripts:

- value of function at point of discontinuity when approaching from negative y-direction
- + value of function at point of discontinuity when approaching from positive y-direction

## THEORY

## General Vortex-Field Relations

The equations relating velocity and vorticity distributions in a slightly perturbed supersonic stream are derived in references 4 and 5. These relations are summarized in the following section. The velocity field is assumed to consist of a major supersonic free-stream velocity  $U$  (taken in the positive x-direction) plus small perturbation velocities  $u$ ,  $v$ , and  $w$  such that the linearized equations of motion are applicable.

Three-dimensional vortex field. - The velocity field in vector form is

$$\bar{q} = (U + u) \bar{i} + v \bar{j} + w \bar{k} \quad (1)$$

The vortex vector field  $\bar{\omega}$  is defined as the curl of the velocity vector. Thus

$$\begin{aligned} \bar{\omega} &= \nabla \times \bar{q} \\ &= \xi \bar{i} + \eta \bar{j} + \zeta \bar{k} \end{aligned} \quad (2)$$

where

$$\xi = \left( \frac{\partial w}{\partial y} - \frac{\partial v}{\partial z} \right)$$

$$\eta = \left( \frac{\partial u}{\partial z} - \frac{\partial w}{\partial x} \right)$$

$$\zeta = \left( \frac{\partial v}{\partial x} - \frac{\partial u}{\partial y} \right)$$

Vortex lines are lines that are tangent at all points to the local vortex vector and are determined from the equation

$$\frac{dx}{\xi} = \frac{dy}{\eta} = \frac{dz}{\zeta} \quad (3)$$

Reference 4 presents the following integral expressions for the perturbation velocities induced by the three-dimensional vortex field:

$$u = -\frac{\beta^2}{2\pi} \sqrt{\int_V \frac{(z_o \eta - y_o \zeta)}{r_o^3} dx_o dy_o dz_o} \quad (4a)$$

$$v = -\frac{\beta^2}{2\pi} \sqrt{\int_V \frac{(x_o \zeta - z_o \xi)}{r_o^3} dx_o dy_o dz_o} \quad (4b)$$

$$w = -\frac{\beta^2}{2\pi} \sqrt{\int_V \frac{(y_o \xi - x_o \eta)}{r_o^3} dx_o dy_o dz_o} \quad (4c)$$

where

$$x_o = x - x_o$$

$$y_o = y - y_o$$

$$z_o = z - z_o$$

$$r_o = \sqrt{x_o^2 + \beta^2 y_o^2 + \beta^2 z_o^2}$$

The subscript  $o$  indicates a variable of integration. The integration is conducted over the volume  $V$  included in the forward Mach cone from the point  $x, y, z$ . That is,

$$x_o \geq \beta \sqrt{y_o^2 + z_o^2}$$

The symbol  $\overline{\int}$  designates the finite part of a divergent integral. (See references 4, 6, or 7.) The procedure for obtaining the finite part is systematized in reference 7 as follows:

The integrals in equations (4a) to (4c) are of the form

$$I = \int_{x_1}^{x_2} \frac{A(x_o)}{(x_2 - x_o)^{3/2}} dx_o \quad (5)$$

The upper limit in equation (5) corresponds to limits on the Mach cone in equations (4a) to (4c). The finite part of this integral is

$$\begin{aligned} \overline{\int I} &= \int_{x_1}^{x_2} \frac{A(x_o)}{(x_2 - x_o)^{3/2}} dx_o \\ &= -J(x_1) - C \end{aligned} \quad (6)$$

where

$$C = \lim_{x_o \rightarrow x_2} \left[ \frac{2A(x_2)}{\sqrt{x_2 - x_o}} - J(x_o) \right] \quad (7)$$

The term  $J(x_o)$  is the indefinite integral of equation (5) and  $J(x_1)$  is the indefinite integral evaluated at the lower limit. The justification for this procedure is presented in references 4, 6, and 7. It can be shown that finite parts are treated in a manner similar to that for ordinary integrals. The rules of addition, differentiation under the integral sign, transformation of variables, and integration by parts apply.

Vortex sheet. - If vorticity exists as a surface of velocity discontinuity in the  $z_o = 0$  plane, then outside this plane,  $\xi$ ,  $\eta$ , and  $\zeta$  are all zero, but in the  $z_o = 0$  plane  $\xi = 0$  whereas  $\xi$  and  $\eta$  are infinite. However, the limits

$$\xi' = \lim_{dz_0 \rightarrow 0} \xi dz_0$$

$$\eta' = \lim_{dz_0 \rightarrow 0} \eta dz_0$$

are finite and are given by (reference 5)

$$\left. \begin{array}{l} \xi' = v_B - v_T \\ \eta' = u_T - u_B \end{array} \right\} \quad (8)$$

The subscripts T and B designate velocities on the top and bottom surfaces of the  $z_0 = 0$  plane, respectively. The perturbation velocities induced by the vortex sheet are obtained by substituting equation (8) in equations (4a) to (4c). In particular, the vertical-perturbation-velocity field (upwash) is given by

$$w = - \frac{\beta^2}{2\pi} \iint_S \frac{Y_0 \xi' - X_0 \eta'}{r_0^3} dx_0 dy_0 \quad (9)$$

The area of integration S includes all the vorticity in the forward Mach cone from x, y, z.

Line vortex. - The vortex lines through all points on an infinitely small closed curve bound a vortex "tube." The circulation

$$\kappa = \omega \sigma$$

(where  $\omega = (\xi^2 + \eta^2 + \zeta^2)^{1/2}$  is the resultant vorticity and  $\sigma$  is the infinitesimal cross-sectional area of the tube) is constant at all points along the tube. The vortex-vector components at any point, in terms of the differential distance  $dl_0$  along the vortex tube, are

$$\xi = \omega \frac{dx_0}{dl_0}$$

$$\eta = \omega \frac{dy_0}{dl_0}$$

$$\zeta = \omega \frac{dz_0}{dl_0}$$

The elemental volume is  $dx_0 dy_0 dz_0 = \sigma dl_0$ . A line vortex is generated by allowing the cross section of the vortex tube to approach zero while maintaining  $\omega_0$  constant. The upwash induced by such a line vortex is found by substituting the preceding expressions into equation (4c) and equals

$$w = -\frac{\beta^2}{2\pi} \int_C \frac{\kappa(y_0 dx_0 - x_0 dy_0)}{r_0^3} \quad (10)$$

where the integration is conducted along the portion of the line vortex within the forecone from  $x, y, z$ . A line vortex cannot terminate within a fluid flow field but must either form a closed curve or extend to infinity or a boundary of the field.

#### Upwash Induced by Line Vortices

Complicated velocity fields can be generated by the linear superposition of relatively simple fields. It will therefore prove useful for subsequent developments to determine the upwash field induced by line vortices of constant slope.

Line vortex of constant slope and strength. - The upwash at  $x, y, z$  due to a line vortex of constant slope  $m$  and strength  $\kappa$ , intersecting the forward Mach cone at  $x_b, y_b$  (fig. 1) is (from equation (10))

$$w = -\frac{\beta^2 \kappa}{2\pi} \int_0^{y_b} \frac{m^2 (y - mx) dy_0}{[(1 - \beta^2 m^2)y_0^2 + 2m(\beta^2 my - x)y_0 + m^2(x^2 - \beta^2 y^2 - \beta^2 z^2)]^{3/2}} \quad (11)$$

The integration is performed in appendix A and yields

$$w = -\frac{\kappa}{2\pi} \frac{(y - mx)(\beta^2 my - x)}{(x^2 - \beta^2 y^2 - \beta^2 z^2)^{1/2} \left[ (y - mx)^2 + (1 - \beta^2 m^2)z^2 \right]} \quad (12)$$

The finite part of the integral in equation (11) is obtained by substituting the lower limit into the indefinite integral (appendix A). No contribution appears from the upper limit. By a translation of coordinates, the upwash due to a line vortex from  $x_1, y_1$  that intersects the forward Mach cone at  $x_b, y_b$  (fig. 2(a)) is found to be

$$w = - \frac{\kappa}{2\pi} \frac{(Y_1 - mX_1)(\beta^2 m Y_1 - X_1)}{r_1 \left[ (Y_1 - mX_1)^2 + (1 - \beta^2 m^2) z^2 \right]} \quad (13)$$

where

$$X_1 = x - x_1$$

$$Y_1 = y - y_1$$

$$r_1 = \sqrt{X_1^2 - \beta^2 Y_1^2 - \beta^2 z^2}$$

By superposition (fig. 2) of a positive line vortex  $\kappa$  from  $x_1, y_1$  and a negative vortex  $-\kappa$  from  $x_2, y_2$ , the upwash due to a line-vortex segment not intersecting the forward Mach cone is

$$w = \frac{\kappa}{2\pi} \left[ G_2(m) - G_1(m) \right] \quad (14)$$

where the notation

$$G_1(m) = \frac{(Y_1 - m_1 X_1)(\beta^2 m_1 Y_1 - X_1)}{r_1 \left[ (Y_1 - m_1 X_1)^2 + (1 - \beta^2 m_1^2) z_1^2 \right]} \quad (15)$$

is used. The subscript for  $G$  indicates the appropriate subscripts for  $X$ ,  $Y$ ,  $Z$ ,  $r$ , and  $m$ .

Equation (14) applies for any line vortex of constant strength and slope. The circulation  $\kappa$  is positive when the vortex vector is in the direction of integration. When the line vortex intersects the forecone, the corresponding limit (infinite  $G_1(m)$  term) is neglected by application of the finite-part concept.

Line vortex of constant slope but varying strength. - Line vortices may coincide to form a resultant line vortex whose circulation is the sum of the strengths of the superposed components.

The general line vortex is then one of variable strength  $\kappa$  along the line  $x_o = x_o(y_o)$  having the local slope  $m_o = dy_o/dx_o$ . The upwash induced by the segment from  $x_1, y_1$  to  $x_2, y_2$  may be written

$$w = -\frac{\beta^2}{2\pi} \int_{y_1}^{y_2} \frac{\kappa(y_o - m_o x_o)}{m_o r_o^3} dy_o \quad (16)$$

The evaluation of equation (16) is generally tedious. For the particular case of constant slope, however, this equation may be integrated by parts to yield a useful expression for upwash. Inasmuch as

$$-\frac{\beta^2(y_o - m_o x_o)}{m_o r_o^3} = \frac{dG_o(m)}{dy_o}$$

the integration by parts gives

$$w = \frac{1}{2\pi} \left( \left[ \kappa_o [G_o(m)] \right]_{y_1}^{y_2} - \int_{y_1}^{y_2} G_o(m) \frac{d\kappa}{dy_o} dy_o \right) \quad (17)$$

The term  $\kappa_o [G_o(m)]$  is disregarded at a limit corresponding to a point on the forward Mach cone.

Equation (17) is a generalization of equation (14) to account for variations in strength along a line vortex of constant slope. Both equations are of fundamental importance because appropriate distributions of such line vortices will be used to simulate a supersonic lifting surface.

#### Characteristics of upwash field due to supersonic line vortex.

1. Infinite line vortices of constant strength and slope. An infinite line vortex inclined supersonically ( $|\beta m| \geq 1$ ) to the free stream is shown in figure 3(a). Because both limits in equation (14) are neglected, the upwash induced by this line vortex is zero. This result agrees with the indications of oblique-airfoil theory because the perturbation velocities are zero downstream of the envelope of the Mach cones from the trailing edge of a two-dimensional airfoil inclined supersonically to the free stream.

The infinite-line vortex along the line  $(y_0 - y_1) = m(x_0 - x_1)$  (fig. 3(b)), inclined subsonically ( $|\beta m| < 1$ ), has one limit that intersects the forward Mach cone whereas the other extends to infinity. The upwash is then, for  $0 \leq \beta m < 1$ ,

$$\begin{aligned} w &= -\frac{\kappa}{2\pi} \lim_{\substack{x_0 \rightarrow -\infty \\ y_0 \rightarrow -\infty}} G_0(m) \\ &= +\frac{\kappa}{2\pi} \frac{\sqrt{1 - \beta^2 m^2} (y_1 - m x_1)}{(y_1 - m x_1)^2 + (1 - \beta^2 m^2) z^2} \end{aligned} \quad (18)$$

where  $x_1, y_1$  is a point on the line vortex. The upwash is infinite along the line vortex. For  $m = 0$ , equation (18) becomes

$$w = +\frac{\kappa}{2\pi} \frac{y_1}{y_1^2 + z^2} \quad (19)$$

which is identical with the expression for upwash due to an infinite vortex parallel to the stream (along the line  $y = y_1$ ) in an incompressible field.

These results indicate that the behavior of the infinite supersonic line vortex for  $|\beta m| \geq 1$  is completely different from that of the incompressible flow vortex. However, when  $|\beta m| < 1$ , both vortices have similar upwash properties in the vicinity of the vortex line and are, in fact, identical for  $m = 0$ .

2. Bent line vortices. The upwash due to a bent line vortex (fig. 3(c)) of constant strength is

$$w = \frac{\kappa}{2\pi} [G_1(m^-) - G_1(m^+)] \quad (20)$$

where  $m_1^-$  and  $m_1^+$  designate the slopes of the line vortex before and after the bend at  $x_1, y_1$ . The term  $r_1$  appears as a factor in the denominator of equation (20) so that the upwash exists only in the aftercone from  $x_1, y_1$  and is infinite on the cone surface (except in the  $z = 0$  plane). This infinite value of upwash is not to be confused with the infinity introduced at the intersection of the line vortex with the forward Mach cone, which is eliminated by application of the finite-part concept.

## Linearized Supersonic-Wing-Theory Relations

The perturbation velocities on supersonic lifting surfaces (zero-thickness wings) have been evaluated for a large variety of plan forms. (See, for example, references 7 to 9.) Those results will now be utilized to determine the vortex field generated by a lifting surface.

Velocity potential. - If the boundary conditions for a lifting surface are specified in the  $z = 0$  plane, the  $u$  and  $v$  velocities are antisymmetric and the  $w$  velocities are symmetric about this plane. Thus the velocities on the top and bottom surface of the  $z = 0$  plane are related by

$$\left. \begin{aligned} u_T &= -u_B \\ v_T &= -v_B \\ w_T &= w_B \end{aligned} \right\} \quad (21)$$

The discontinuities in  $u$  and  $v$  constitute a vortex sheet. Because the flow is everywhere irrotational, except across this sheet, a perturbation-velocity potential  $\phi$  can be so defined that

$$\left. \begin{aligned} d\phi &= \frac{\partial \phi}{\partial x} dx + \frac{\partial \phi}{\partial y} dy + \frac{\partial \phi}{\partial z} dz \\ &= u dx + v dy + w dz \end{aligned} \right\} \quad (22)$$

When the undisturbed flow field upstream of the wing is considered to be of zero potential, and the boundary condition requiring that  $u_T = u_B = 0$  off the wing (antisymmetry of  $u$  and zero lift off wing) is applied, the potential in the  $z = 0$  plane may be obtained by integrating along lines of constant  $y$ .

$$\left. \begin{aligned} \phi_T &= \int_{x_l}^x u_T dx \\ \phi_B &= \int_{x_l}^x u_B dx \end{aligned} \right\} \quad (23)$$

where  $x_l$  is the equation of the leading edge as a function of  $y$ . From equation (23) it may be concluded that

1. Everywhere in  $z = 0$  plane except behind the wing leading edge  $\varphi_T = \varphi_B = 0$ .

2. At a given span station  $\varphi_T$  and  $\varphi_B$  remain constant for all values of  $x$  downstream of the trailing edge.

Lines of constant potential for rectangular and triangular wings are shown in figure 4.

Vortex lines. - The equation for the vortex lines (from equation (3)) is

$$\eta' dx - \xi' dy = 0 \quad (24)$$

When the following expressions (equations (8), (21), and (22)) are substituted

$$\xi' = -(v_T - v_B) = -2 \frac{\partial \varphi_T}{\partial y} = 2 \frac{\partial \varphi_B}{\partial y}$$

$$\eta' = u_T - u_B = 2 \frac{\partial \varphi_T}{\partial x} = -2 \frac{\partial \varphi_B}{\partial x}$$

the equation for the vortex lines becomes

$$\frac{\partial \varphi_T}{\partial x} dx + \frac{\partial \varphi_T}{\partial y} dy = \frac{\partial \varphi_B}{\partial x} dx + \frac{\partial \varphi_B}{\partial y} dy = 0 \quad (25)$$

Comparison with equation (22) shows that equation (25) represents lines of constant potential. Thus the vortex lines coincide with the lines of constant potential in the  $z = 0$  plane.

Circulation. - The circulation included between two points  $x_1, y_1$  and  $x_2, y_2$  on a wing is given by

$$\kappa = \oint u dx + v dy + w dz \quad (26)$$

The path of integration is arbitrary except that the path should cross the  $z = 0$  plane only at the two specified points. If the integral is taken along the top and bottom surfaces of the  $z = 0$  plane,

$$\begin{aligned}
 \kappa &= \int_{x_1, y_1}^{x_2, y_2} (u_T dx + v_T dy) + \int_{x_2, y_2}^{x_1, y_1} (u_B dx + v_B dy) \\
 &= (\varphi_{T,2} - \varphi_{T,1}) + (\varphi_{B,1} - \varphi_{B,2}) = \Delta\varphi_2 - \Delta\varphi_1 \quad (27)
 \end{aligned}$$

where  $\Delta\varphi$  equals  $\varphi_T - \varphi_B$  and represents the jump in potential at the point. The quantity  $\Delta\varphi$  is, in fact, the doublet potential (reference 2), so that the net circulation between two points equals the difference in the doublet potential between those points. The equivalence of a doublet distribution and a vortex distribution indicates that the flow about a lifting surface can be calculated on either basis.

Circulation and lift. - The lift per unit span is given by the chordwise integration

$$L(y) = \frac{1}{2} \rho U^2 \int_{x_l}^{x_t} (c_{p,B} - c_{p,T}) dx \quad (28)$$

After substitution of the linearized values for pressure coefficient

$$c_{p,T} = - \frac{2u_T}{U} = - \frac{2}{U} \frac{\partial \varphi_T}{\partial x}$$

$$c_{p,B} = - \frac{2u_B}{U} = - \frac{2}{U} \frac{\partial \varphi_B}{\partial x}$$

and integration, equation (28) becomes, because  $\Delta\varphi_l = 0$ ,

$$L(y) = \rho U \Delta\varphi_t \quad (29)$$

The factor  $\Delta\varphi_t$  is the circulation included between the leading and trailing edges at the spanwise station under consideration. When this circulation is designated  $\Gamma$ , equation (29) becomes

$$L(y) = \rho U \Gamma \quad (30)$$

which is the familiar incompressible-flow relation. Also

$$\begin{aligned}
 \frac{d\Gamma}{dy} &= \frac{d(\varphi_T - \varphi_B)_t}{dy} \\
 &= (v_T - v_B)_t \\
 &= -(\xi')_t
 \end{aligned} \tag{31}$$

Equation (31) relates the shed vorticity to the rate of change of spanwise loading.

#### APPLICATIONS TO CALCULATIONS OF SUPERSONIC DOWNWASH

The vertical perturbation velocities due to a supersonic line vortex of constant slope have been presented in a form that permits analytical or mechanical evaluation (equations (14) and (17)). The vortex distribution associated with a lifting surface has also been discussed. These relations will be used to develop exact and approximate methods for calculating downwash behind lifting surfaces at supersonic speeds.

##### Downwash an Infinite Distance behind Wing

The vertical-perturbation-velocity field behind a supersonic lifting surface (from equation (9)) is

$$\begin{aligned}
 w &= -\frac{\beta^2}{2\pi} \sqrt{\int_{S_p} \frac{(Y_O \xi' - X_O \eta')}{r_O^3} dx_O dy_O} - \\
 &\quad \frac{\beta^2}{2\pi} \sqrt{\int_{S_w} \frac{Y_O \xi'}{r_O^3} dx_O dy_O}
 \end{aligned} \tag{32}$$

where the integration over the plan form is designated by  $S_p$  and over the wake by  $S_w$ . As  $x$  becomes infinite,  $X_O$  also becomes

infinite in the integral for the bound (plan form) vortices. This integral then becomes zero because  $X_0$  is of higher order in the denominator than in the numerator. Thus, only the integration over the trailing vortex sheet contributes to the vertical perturbation velocities at infinity. The trailing vortex sheet may be considered to consist of elemental vortices of infinite length along  $y = \text{constant}$  lines, each having the strength

$d\kappa = \xi' dy_0 = - \frac{d\Gamma}{dy_0} dy_0$ . The vertical perturbation velocity at  $\infty, y, z$  due to the elemental vortex along  $y = y_0$  is, from equation (19)

$$dw = \frac{\left( - \frac{d\Gamma}{dy_0} dy_0 \right)}{2\pi} \frac{y_0}{y_0^2 + z^2}$$

so that the vertical-perturbation-velocity field at infinity is given by

$$w = - \frac{1}{2\pi} \int_{-\frac{b}{2}}^{\frac{b}{2}} \frac{y_0}{y_0^2 + z^2} \frac{d\Gamma}{dy_0} dy_0 \quad (33)$$

where  $b/2$  is the semispan. The velocity field obtained from equation (33) is identical to that induced by a subsonic wing with the given span loading. The velocity field at infinity is thus independent of Mach number (excluding the influence of Mach number on  $d\Gamma/dy_0$ ). This result has been derived in references 1 and 2 by other methods. The evaluation of equation (33) is relatively simple and may be used to approximate the downwash several chords behind a supersonic wing.

#### Regions of Infinite Downwash

Approximate solutions may modify or introduce singularities in the downwash field. It is therefore of interest to establish the regions for which linearized theory indicates an infinite downwash.

Infinite downwash in  $z = 0$  plane. - The vertical perturbation velocities in the  $z = 0$  plane that exist an infinite

distance behind a wing having a discontinuity in  $d\Gamma/dy_o$  will first be considered. These velocities are determined from the equation

$$w = -\frac{1}{2\pi} \int_{-\frac{b}{2}}^{\frac{b}{2}} \frac{d\Gamma/dy_o}{y_o} dy_o \quad (34)$$

The Cauchy principal value is required for points on the vortex sheet. For the particular case of triangular loading (fig. 5(a))

$$\frac{d\Gamma}{dy_o} = \frac{2\Gamma_m}{b}$$

in the integration interval  $-\frac{b}{2} \leq y_o \leq 0$  and

$$\frac{d\Gamma}{dy_o} = -\frac{2\Gamma_m}{b}$$

in the interval  $0 \leq y_o \leq \frac{b}{2}$  ( $\Gamma_m$  is the circulation at the midspan).

When these values for  $\frac{d\Gamma}{dy_o}$  are substituted in equation (34), the integral yields

$$w = \frac{\Gamma_m}{\pi b} \log_e \left| \frac{y^2}{y^2 - \frac{b^2}{4}} \right| \quad (35)$$

Infinite upwash exists along the lines  $y = \pm b/2$  whereas infinite downwash exists along the line  $y = 0$ . These infinite values are due to the discontinuities in the spanwise vorticity distribution and apply for all points on these lines downstream of the wing trailing edge.

In general, if  $(d\Gamma/dy_o)^-$  and  $(d\Gamma/dy_o)^+$  represent a discontinuity in the rate of change of spanwise loading at station  $y = y_1$ , infinite vertical perturbation velocities will exist along  $y = y_1$  downstream of the trailing edge. For  $(d\Gamma/dy_o)^- < (d\Gamma/dy_o)^+$  infinite upwash will exist, and for  $(d\Gamma/dy_o)^- > (d\Gamma/dy_o)^+$  infinite

downwash will exist along this line. Such discontinuities in  $d\Gamma/dy_0$  originate both at a wing tip and at those points along a supersonic trailing edge where the plan-form slope is discontinuous and the local-wing-pressure coefficient is not equal to zero. This discontinuity in vorticity may be verified by the methods employed in reference 1 for finding the upwash and sidewash directly behind a supersonic trailing edge.

The discontinuity in shed vorticity at the tips of an elliptically loaded wing is a special case of the previously stated rule governing infinite vertical perturbation velocities in the  $z = 0$  plane. For wing loading given by

$$\Gamma = \Gamma_m \sqrt{1 - \frac{4}{b^2} y_0^2}$$

the shed vorticity is

$$\frac{d\Gamma}{dy_0} = \frac{-\frac{4}{b^2} \Gamma_m y_0}{\sqrt{1 - \frac{4}{b^2} y_0^2}}$$

and the vertical-perturbation-velocity field at infinity, in the  $z = 0$  plane, is

$$w = \frac{2\Gamma_m}{\pi b^2} \int_{-\frac{b}{2}}^{\frac{b}{2}} \frac{y_0 dy_0}{y_0 \sqrt{1 - \frac{4}{b^2} y_0^2}}$$

Integration yields

$$w = -\frac{\Gamma_m}{b}$$

for

$$|y| < \frac{b}{2}$$

and

$$w = - \frac{\Gamma_m}{b} \left( 1 - \frac{|y|}{\sqrt{y^2 - \frac{b^2}{4}}} \right)$$

for

$$|y| \geq \frac{b}{2}$$

As indicated in figure 5(b), the vertical perturbation velocity is discontinuous at  $y = \pm b/2$ , but is bounded for all points on the vortex sheet.

Infinite downwash on Mach cone from wing tip. - Reference 3 indicates infinite vertical perturbation velocities on the downstream Mach cones from the tips of a triangular wing. This result will now be extended to apply to any wing tip formed by the intersection of a subsonic leading edge and a supersonic trailing edge provided that the slope of the subsonic edge is not zero at the tip (fig. 6).

The contribution to the vertical-perturbation-velocity field due to the bending of an elemental vortex at the trailing edge (fig. 6) is, from equation (20),

$$dw = - \frac{\frac{d\Gamma}{dy_o} dy_o}{2\pi} [G_o(m^-) - G_o(0)] \quad (36)$$

where

$$G_o(0) = \frac{-1}{r_o} \frac{x_o y_o}{(y_o^2 + z_o^2)}$$

The vertical perturbation velocity at a point on the Mach cone from this tip due to the bending of the vortices is found by integrating (along the trailing edge)

$$w = - \frac{1}{2\pi} \int_{y_a}^0 [G_o(m^-) - G_o(0)] \frac{d\Gamma}{dy_o} dy_o \quad (37)$$

Equation (37) in the expanded form becomes

$$w = -\frac{1}{2\pi} \int_{y_a}^0 \left[ \frac{(Y_o - m_o^- X_o)(\beta^2 m_o^- Y_o - X_o)}{(Y_o - m_o^- X_o)^2 + (1 - \beta^2 m_o^- 2)z^2} + \frac{X_o Y_o}{Y_o^2 + z^2} \right] \frac{1}{r_o} \frac{d\Gamma}{dy_o} dy_o \quad (38)$$

The limits of integration are roots of  $r_o$ , so that the factor  $1/r_o$  is singular of order 1/2 at the limits and the integral is improper (assuming  $(m_o^-)_{Y_o=0} \neq 0$ ). The convergence of the integral depends on the nature of  $d\Gamma/dy_o$  at the limits. Appendix B shows, however, that  $d\Gamma/dy_o$  is also singular of order 1/2 at the tip. The combined singularity causes equation (38) to diverge at the upper limit and results in logarithmically infinite vertical perturbation velocities on the Mach cone from the tip. The divergence is a consequence of both the singularity in  $d\Gamma/dy_o$  and the singularity on the Mach cone from a bend in the elemental line vortex.

The infinite vertical perturbation velocities on the Mach cone from the tip do not appear in the  $z = 0$  plane inasmuch as equation (38) then reduces to

$$w = \frac{1}{2\pi} \int_{y_a}^0 \frac{m_o^- \sqrt{X_o^2 - \beta^2 Y_o^2}}{(Y_o - m_o^- X_o) Y_o} \frac{d\Gamma}{dy_o} dy_o$$

and the singularity due to  $r_o$  is no longer present.

#### Approximate Downwash Solutions

Several approximate methods for obtaining downwash were considered. Methods based on a lifting line seem the most promising and are discussed in the following sections. A bent lifting line is proposed for determining the downwash behind a swept wing and an unbent lifting line (horseshoe vortex system) for determining the downwash behind an unswept wing. These methods are applied to compute the downwash behind triangular and rectangular wings and the results are compared with the exact linearized solutions.

A lifting line concentrates the chordwise loading into a line. Thus the bound circulation is represented by a line vortex of variable strength ( $\kappa = \Gamma = \Delta p_t$ ), whereas the trailing-vortex system maintains the same vorticity ( $\xi' = -d\Gamma/dy_o$ ) but now originates at the line rather than at the trailing edge.

Bent lifting line. - A lifting line approximating the section centers of pressure

$$x_{cp} = x_l + \frac{\int_{x_l}^{x_t} (C_{p,B} - C_{p,T})(x - x_l) dx}{\int_{x_l}^{x_t} (C_{p,B} - C_{p,T}) dx}$$

seems to be a reasonable representation of a sweptback or swept-forward wing. In order to facilitate downwash calculations, the line of section centers of pressure can be approximated by two straight-line segments, each connecting an end point to the midpoint of the line. The result is a bent lifting line (fig. 7) of span  $b$  and effective chord  $c_e$  ( $x$ -distance between midpoint and end points of lifting line). For a sweptback lifting line, the slopes at the midpoint are

$$(m_o^-)_{y_o=0} = -\frac{b}{2c_e}$$

and

$$(m_o^+)_{y_o=0} = \frac{b}{2c_e}$$

The vertical perturbation velocities induced by the bound vortices can be determined from equation (17) and equal

$$w = \frac{\Gamma_m}{2\pi} \left[ G_o(m^-) - G_o(m^+) \right]_{y_o=0} - \frac{1}{2\pi} \int_{y_a}^{y_b} G_o(m) \frac{d\Gamma}{dy_o} dy_o \quad (39)$$

where the integration is conducted along the lifting line (figs. 8(a) and 8(b)). The vertical perturbation velocities induced by the trailing-vortex system are obtained from

$$w = \frac{1}{2\pi} \int_{y_a}^{y_b} G_o(0) \frac{d\Gamma}{dy_o} dy_o \quad (40)$$

The term  $G_o(0)$  is as defined for equation (36) and the integration is again conducted along the lifting line. The vertical perturbation velocities induced by the complete lifting-line system (bound and trailing vortices) are then the sum of equations (39) and (40) and equal

$$w = \frac{\Gamma_m}{2\pi} [G_o(m^-) - G_o(m^+)]_{y_o=0} - \frac{1}{2\pi} \int_{y_a}^{y_b} [G_o(m) - G_o(0)] \frac{d\Gamma}{dy_o} dy_o \quad (41)$$

The value  $m_o = (m_o^-)_{y_o=0}$  is used for the integration interval  $y_a \leq y_o \leq 0$  and  $m_o = (m_o^+)_{y_o=0}$  is used for the interval  $0 \leq y_o \leq y_b$ .

Equation (41) is the expression for the vertical perturbation velocities behind a swept wing using the bent-lifting-line approximation. This equation can also be considered as derived from a superposition of a system of bent line vortices of constant strength (equation (20)), as indicated in figure 9. The nonintegral term of equation (41) is then the contribution of the bent line vortex of strength  $\Gamma_m$  whereas the integral term represents the contribution of the elemental line vortices of strength  $-\frac{d\Gamma}{dy_o} dy_o$ .

The integral term of equation (41) may be evaluated by analytical or mechanical methods. When mechanical methods are used, the singularities in the integrand must be isolated. Suitable procedures for isolating the commonly encountered singularities are as follows:

(1) Singularity due to intersection of forward Mach cone with lifting line. The integrand in equation (41) is infinite at the intersection of the forward Mach cone and the lifting line (for  $z \neq 0$ ). The contribution  $\delta w$  of the integral, for the interval  $y_b - \epsilon_b \leq y_o \leq y_b$  (fig. 8(a)), to the vertical perturbation velocity field may be written

$$\delta w = -\frac{1}{2\pi} \int_{y_b - \epsilon_b}^{y_b} \left( \left[ G_o(m) - G_o(0) \right] r_o \frac{dr}{dy_o} - \left[ \left[ G_o(m) - G_o(0) \right] r_o \frac{dr}{dy_o} \right]_{y_o=y_b} \right) \frac{dy_o}{r_o} -$$

$$\frac{1}{2\pi} \left\{ \left[ G_o(m) - G_o(0) \right] r_o \frac{dr}{dy_o} \right\}_{y_o=y_b} \int_{y_b - \epsilon_b}^{y_b} \frac{dy_o}{r_o} \quad (42)$$

where  $\epsilon_b$  is a convenient length. The first integral in equation (42) is proper and may be mechanically evaluated. The second integral is,

for

$$0 < \beta m_o < 1,$$

$$\int_{y_b - \epsilon_b}^{y_b} \frac{dy_o}{r_o} = \left\{ \frac{m_o}{\sqrt{1 - \beta^2 m_o^2}} \log_e \left[ m_o \sqrt{1 - \beta^2 m_o^2} r_o + (1 - \beta^2 m_o^2) y_o - m_o (x - \beta^2 m_o y) \right] \right\}_{y_b - \epsilon_b}^{y_b} = \frac{2m_o}{\sqrt{1 - \beta^2 m_o^2}} \sinh^{-1} \sqrt{\frac{(1 - \beta^2 m_o^2) \epsilon_b}{2 [m_o (x - \beta^2 m_o y) - (1 - \beta^2 m_o^2) y_b]}}$$

for

$$\beta m_o > 1,$$

$$\int_{y_b - \epsilon_b}^{y_b} \frac{dy_o}{r_o} = \left[ \frac{m_o}{\sqrt{\beta^2 m_o^2 - 1}} \sin^{-1} \sqrt{\frac{m_o(x - \beta^2 m_o y) - (1 - \beta^2 m_o^2) y_o}{\beta m_o \sqrt{(y - m_o x)^2 + (1 - \beta^2 m_o^2) z^2}}} \right]_{y_b - \epsilon_b}^{y_b}$$

$$= \frac{2m_o}{\sqrt{\beta^2 m_o^2 - 1}} \sin^{-1} \sqrt{\frac{(\beta^2 m_o^2 - 1) \epsilon_b}{2 [m_o(x - \beta^2 m_o y) - (1 - \beta^2 m_o^2) y_b]}}$$

for

$$\beta m_o = 1,$$

$$\int_{y_b - \epsilon_b}^{y_b} \frac{dy_o}{r_o} = \left[ \frac{m_o \sqrt{2(y - m_o x) y_o + m_o^2 x^2 - y^2 - z^2}}{y - m_o x} \right]_{y_b - \epsilon_b}^{y_b}$$

$$= m_o \sqrt{\frac{2\epsilon_b}{m_o x - y}}$$

where  $m_o$  is the slope of the lifting line at  $y_b$ . A similar procedure applies for the singularity at  $y_a$ .

(2) Singularity in  $dI/dy_o$  at wing tip. The vertical perturbation velocity at a point whose forward Mach cone intersects the edges of the trailing vortex sheet (fig. 8(b)) is obtained from equation (41) by integration between the limits  $-\frac{b}{2} \leq y_o \leq \frac{b}{2}$ . If  $dI/dy_o$  is singular at these limits, the singularity may be isolated by a procedure similar to that used in equation (42). Thus, the contribution to the vertical perturbation velocity field, from the integration interval  $\frac{b}{2} - \epsilon_b \leq y_o \leq \frac{b}{2}$ , may be written

$$\begin{aligned}
 \delta w &= -\frac{1}{2\pi} \int_{\frac{b}{2} - \epsilon_b}^{\frac{b}{2}} \left[ G_o(m) - G_o(0) \right] \frac{d\Gamma}{dy_o} dy_o \\
 &= -\frac{1}{2\pi} \int_{\frac{b}{2} - \epsilon_b}^{\frac{b}{2}} \left( \left[ G_o(m) - G_o(0) \right] - \left\{ \left[ G_o(m) - G_o(0) \right] \right\}_{y_o = \frac{b}{2}} \right) \frac{d\Gamma}{dy_o} dy_o - \\
 &\quad \frac{1}{2\pi} \left\{ \left[ G_o(m) - G_o(0) \right] \right\}_{y_o = \frac{b}{2}} \int_{\frac{b}{2} - \epsilon_b}^{\frac{b}{2}} \frac{d\Gamma}{dy_o} dy_o
 \end{aligned} \tag{43}$$

where

$$\int_{\frac{b}{2} - \epsilon_b}^{\frac{b}{2}} \frac{d\Gamma}{dy_o} dy_o = -(\Gamma)_{y_o = \frac{b}{2}} = -\epsilon_b$$

(3) Singularity at points on vortex sheet. The Cauchy principal value of the integral (equation (41)) is required for determining the vertical perturbation velocity at a point on the vortex

sheet  $z = 0$ ,  $-\frac{b}{2} \leq y \leq \frac{b}{2}$ . For this case, considering the interval  $y - \epsilon \leq y_o \leq y + \epsilon$  (fig. 8(c)), the contribution of the integral to the vertical-perturbation-velocity field is

$$\delta w = +\frac{1}{2\pi} \int_{y - \epsilon}^{y + \epsilon} \frac{m_o \sqrt{x_o^2 - \beta^2 y_o^2}}{(y_o - m_o x_o) y_o} \frac{d\Gamma}{dy_o} dy_o \tag{44}$$

If  $d\Gamma/dy_o$  can be approximated by the first two terms of the Taylor's expansion

$$\frac{d\Gamma}{dy_o} \approx \left( \frac{d\Gamma}{dy_o} \right)_{y_o = y} + (y_o - y) \left( \frac{d^2\Gamma}{dy_o^2} \right)_{y_o = y}$$

and  $\epsilon$  is sufficiently small that

$$\frac{m_o \sqrt{x_o^2 - \beta^2 y_o^2}}{(Y_o - m_o x_o)} \approx -1$$

equation (44) may be written

$$\begin{aligned} \delta w &= -\frac{1}{2\pi} \int_{y - \epsilon}^{y + \epsilon} \left[ \left( \frac{d\Gamma}{dy_o} \right)_{y_o = y} - Y_o \left( \frac{d^2\Gamma}{dy_o^2} \right)_{y_o = y} \right] \frac{dy_o}{Y_o} \\ &= + \frac{\epsilon}{\pi} \left( \frac{d^2\Gamma}{dy_o^2} \right)_{y_o = y} \end{aligned} \quad (45)$$

Inasmuch as  $d\Gamma/dy_o$  is an odd function in  $y_o$  for a wing symmetrical about the midspan,  $d\Gamma/dy_o$  is either discontinuous or zero for  $y_o = 0$ . If  $d\Gamma/dy_o$  is discontinuous, the vertical perturbation velocities are infinite along this line.

Unbent lifting line. - The unbent lifting line (horseshoe-vortex system) appears to be a reasonable representation for an upswept wing. The use of such a lifting line considerably simplifies the calculations.

The vertical perturbation velocities induced by an unbent lifting line (along the  $y$ -axis) are obtained from equation (41) by setting  $m_o = \infty$  and are equal to

$$w = -\frac{1}{2\pi} \int_{y_a}^{y_b} \frac{x Y_o (r_o^2 - \beta^2 z^2)}{r_o (x^2 - \beta^2 z^2) (Y_o^2 + z^2)} \frac{d\Gamma}{dy_o} dy_o \quad (46)$$

The singularities are isolated as follows:

(1) Singularity due to intersection of forward Mach cone with lifting line.

$$\delta w = -\frac{1}{2\pi} \int_{y_b - \epsilon_b}^{y_b} \left[ \frac{x Y_o (r_o^2 - \beta^2 z^2)}{(x^2 - \beta^2 z^2)(Y_o^2 + z^2)} \frac{d\Gamma}{dy_o} + \left( \frac{\beta^2 z^2}{x Y_o} \frac{d\Gamma}{dy_o} \right)_{y_o=y_b} \right] \frac{dy_o}{r_o} +$$

$$\frac{1}{2\pi} \left( \frac{\beta^2 z^2}{x Y_o} \frac{d\Gamma}{dy_o} \right)_{y_o=y_b} \int_{y_b - \epsilon_b}^{y_b} \frac{dy_o}{r_o}$$

where

$$\int_{y_b - \epsilon_b}^{y_b} \frac{dy_o}{r_o} = \frac{2}{\beta} \sin^{-1} \sqrt{\frac{\epsilon_b}{2(y_b - y)}}$$

(2) Singularity in  $d\Gamma/dy_o$  at the tip.

$$\delta w = \frac{-1}{2\pi} \int_{\frac{b}{2} - \epsilon_b}^{\frac{b}{2}} \left\{ \frac{x Y_o (r_o^2 - \beta^2 z^2)}{r_o (x^2 - \beta^2 z^2)(Y_o^2 + z^2)} - \left[ \frac{x Y_o (r_o^2 - \beta^2 z^2)}{r_o (x^2 - \beta^2 z^2)(Y_o^2 + z^2)} \right]_{y_o=\frac{b}{2}} \right\} \frac{d\Gamma}{dy_o} dy_o +$$

$$\frac{1}{2\pi} \left[ \frac{x Y_o (r_o^2 - \beta^2 z^2)}{r_o (x^2 - \beta^2 z^2)(Y_o^2 + z^2)} \right]_{y_o=\frac{b}{2}} \stackrel{(\Gamma)}{=} \frac{b}{2} - \epsilon_b$$

(3) Singularity at points on vortex sheet.

$$\delta w = \frac{\epsilon}{\pi} \left( \frac{d^2 \Gamma}{dy_o^2} \right)_{y_o=y}$$

The chordwise location of the unbent lifting line that will give the best average agreement with the exact linearized solution is still to be determined. According to the techniques used in subsonic-wing theory, an unbent lifting line at the wing center of pressure should be a good first approximation. However, further investigation is required. It may be possible to determine the best location for each general class of plan forms by comparing the lifting-line solution with the exact linearized solution for several representative plan forms.

Examples and discussion. - A bent lifting line and an unbent lifting line will be used to obtain solutions for the downwash in the  $y = 0$  plane behind triangular wings having subsonic leading edges. The chordwise distribution of wing loading suggests the use of the bent lifting line. The unbent lifting line will be used for purposes of comparison. An unbent lifting line also will be used to compute the downwash in the  $y = 0$  plane behind rectangular wings. The chordwise location of the unbent lifting line giving the best average agreement with the exact linearized solutions will be noted for both the triangular and the rectangular wings. In order to simplify the expressions,  $M = \sqrt{2}$  (that is,  $\beta = 1$ ) will be assumed.

The spanwise circulation distribution for a triangular wing of span  $b$  and root chord  $c_r$ , having subsonic  $\left(\frac{b}{2c_r} < 1\right)$  leading edges, is (from equation (24) of reference 2)

$$\Gamma = \Delta \varphi_t = \frac{\alpha U b}{E} \sqrt{1 - \frac{4}{b^2} y_0^2}$$

where  $E$  is the complete elliptic integral of the second kind

with modulus  $\sqrt{1 - \left(\frac{b}{2c_r}\right)^2}$ . The circulation at the midspan is

$$\Gamma_m = \frac{\alpha U b}{E}$$

and the rate of change of circulation is

$$\frac{d\Gamma}{dy_0} = - \frac{4\alpha U}{Eb} \frac{y_0}{\sqrt{1 - \frac{4y_0^2}{b^2}}}$$

The expression for the vertical perturbation velocities in the  $y = 0$  plane using the bent-lifting-line approximation of figure 10(a) is

$$w = -\frac{\alpha U b}{\pi E} \left[ G_o(m^+) \right]_{y_o=0} + \frac{4\alpha U}{\pi b E} \int_0^{y_b} \frac{[G_o(m^+) - G_o(0)]}{\sqrt{1 - \frac{4}{b^2} y_o^2}} y_o dy_o \quad (47)$$

where  $(m_o^+)_{y_o=0} = \frac{b}{c_r}$ . Equation (47) is obtained from equation (41) and the properties of an even function. The vertical-perturbation-velocity field behind an unbent lifting line, having the same loading (fig. 10(b)) is from equation (46),

$$w = -\frac{4\alpha U}{\pi b E} \int_0^{y_b} \frac{x(r_o^2 - z^2) y_o^2 dy_o}{r_o(x^2 - z^2)(y_o^2 + z^2) \sqrt{1 - \frac{4}{b^2} y_o^2}} \quad (48)$$

The spanwise circulation for a rectangular wing of aspect ratio  $\frac{b}{c_r} \geq 2$  for the tip region  $\frac{b}{2} - c_r \leq y_o \leq \frac{b}{2}$  is

$$\Gamma = \Delta \Phi_t = \frac{4\alpha U}{\pi} \left[ \sqrt{(y_o + c_r - \frac{b}{2})(\frac{b}{2} - y_o)} + c_r \tan^{-1} \sqrt{\frac{\frac{b}{2} - y_o}{y_o + c_r - \frac{b}{2}}} \right] \quad (49a)$$

and for  $0 \leq y_o \leq \frac{b}{2} - c_r$

$$\Gamma = 2\alpha U c_r \quad (49b)$$

Equations (49a) and (49b) were obtained from equation (20) of reference 8. The wing is illustrated in figure 10(c). The rate of change of spanwise circulation for  $\frac{b}{2} - c_r \leq y_o \leq \frac{b}{2}$  is

$$\frac{d\Gamma}{dy_0} = -\frac{4\alpha U}{\pi} c_r \sqrt{\frac{y_0 + c_r - \frac{b}{2}}{\frac{b}{2} - y_0}}$$

The vertical-perturbation-velocity field in the  $y = 0$  plane behind an unbent lifting line having this loading is

$$w = -\frac{4\alpha U c_r}{\pi^2} \int_{\frac{b}{2} - c_r}^{\frac{b}{2}} \frac{x (r_0^2 - z^2) y_0}{r_0 (x^2 - z^2) (y_0^2 + z^2)} \sqrt{\frac{y_0 + c_r - \frac{b}{2}}{\frac{b}{2} - y_0}} dy_0 \quad (50)$$

Equation (47) was evaluated to determine the downwash along the line  $y = 0$ ,  $z = 0$  and along the line  $y = 0$ ,  $z = 0.1 b$  for triangular wings with aspect ratios  $(2b/c_r)$  of 1.6 and 3.2. Equation (48) was evaluated for the same wings at points along the line  $y = 0$ ,  $z = 0$ . Equation (50) was evaluated at points along the line  $y = 0$ ,  $z = 0$  for rectangular wings with aspect ratios  $(b/c_r)$  of 2 and 4. The integrations were performed mechanically for equations (47) and (50) and analytically for equation (48). The results are compared with the exact linearized solutions obtained from references 1 to 3 in figures 11 to 14.

The bent-lifting-line solutions for the triangular wings are shown in figures 11 and 12. The discontinuity in the curves for the  $z = 0.1 b$  plane (figs. 11(b) and 12(b)) designates large negative (upwash) values that become infinite on the Mach cone from the tip, as indicated in the discussion associated with equation (38). The agreement with the exact solutions is good for all points except those within  $1/2$  chord from the trailing edge. The correlation is unexpected because of the large contribution of the nonintegral term of equation (47). This term is associated with the bending of the lifting line at the midpoint. This bend was artificially introduced. The agreement with the exact downwash solutions, however, indicates that the bent lifting line is a good average representation of the triangular-type wing (at least in regard to the downwash solution in the region of the line  $y = 0$ ,  $z = 0$ ). This method should give even better agreement when used to represent a sweptback wing such as the one represented in figure 7, because the bent lifting line would then more closely approximate the actual vorticity distribution.

The unbent-lifting-line solution for the triangular wings is presented in figure 13. The lifting line is placed at the 3/4-chord point to give the best average agreement with the exact linearized solution. (The center of pressure for these wings is at the 2/3-chord point.) The agreement is not as good as that obtained with the bent lifting line and indicates that the bent line is more suitable for computing downwash behind triangular wings. The smaller-aspect-ratio wing ( $2b/c_r = 1.6$ ) is in better agreement with the exact linearized solution because of the rapidity with which the downwash approaches the asymptotic value at infinity.

The unbent-lifting-line solution for the rectangular wings is presented in figure 14. The downwash obtained with the lifting line at the 1/2-chord point is in excellent agreement with the exact linearized solution. (The location of the center of pressure is at the 4/9-chord and 10/21-chord points for aspect ratios of 2 and 4, respectively.) These calculations suggest that the unbent lifting line is well suited for computing the downwash behind unswept supersonic wings and that the best chordwise position for the unbent lifting line is at or slightly downstream of the wing center of pressure.

A more accurate estimate of the downwash in the  $z = 0$  plane close to the trailing edge may be obtained by judiciously fairing the curve obtained by the line-vortex method to the known value of downwash at the trailing edge. At a subsonic trailing edge satisfying the Kutta condition,  $-w/cU$  is unity; whereas at a supersonic trailing edge,  $-w/cU$  can be computed by the method presented in reference 1.

It should be noted that linearized theory neglects the effect on the downwash of the friction wake and the displacement and distortion of the trailing vortex sheet. An experimental program, such as that reported in reference 10 for wings in subsonic flight, is ultimately required to determine the necessary modifications to linearized theory that will result in good agreement between theory and practice.

#### SUMMARY OF ANALYSIS AND APPLICATIONS

The perturbation field induced by a line vortex in a supersonic stream and the downwash field behind a supersonic lifting surface have been examined for the purpose of establishing approximate methods for the calculation of supersonic downwash.

An infinite line vortex of constant strength and slope, supersonically inclined to the free stream, induces no perturbation field. A subsonically inclined line vortex has properties similar to those of a vortex in an incompressible-flow field. Bends in a line vortex induce infinite vertical perturbation velocities on the surface of the downstream Mach cone from the bend (except in the  $z = 0$  plane).

The downwash field behind a supersonic lifting surface differs from that behind a subsonic wing in several respects. For a supersonic lifting surface, discontinuities in shed vorticity occur at those points along a supersonic trailing edge where the plan-form slope is discontinuous and the local pressure coefficient is not zero. These discontinuities lead to singularities in the downwash field in the  $z = 0$  plane. Also, the vertical perturbation velocities are logarithmically infinite on the downstream Mach cone from a wing tip formed by the intersection of a subsonic leading plan-form edge and a supersonic trailing plan-form edge.

A bent-lifting-line method has been proposed for the solution of the downwash field behind swept wings. When applied to a triangular wing, this method gave results that were in very good agreement with the exact linearized solution for points near the line  $y = 0$ ,  $z = 0$  except for points within  $1/2$  chord of the wing trailing edge.

An unbent lifting line (horseshoe-vortex system) has been proposed for unswept wings. This method was applied to determine the downwash behind rectangular wings with aspect ratios  $b/c_r$  of 2 and 4. Excellent agreement was obtained for both aspect ratios by placing the lifting line at the  $1/2$ -chord point.

Lewis Flight Propulsion Laboratory,  
National Advisory Committee for Aeronautics,  
Cleveland, Ohio, April 29, 1949.

## APPENDIX A

## UPWASH INDUCED BY LINE VORTEX

The upwash induced by the line vortex segment of figure 1 is,

$$w = -\frac{\beta^2 \kappa}{2\pi} \int_0^{y_b} \frac{m^2(y-mx)dy_o}{[(1-\beta^2 m^2)y_o^2 + 2m(\beta^2 my - x)y_o + m^2(x^2 - \beta^2 y^2 - \beta^2 z^2)]^{3/2}} \quad (11)$$

The upper limit is at the intersection of the line vortex ( $y_o = mx_o$ ) with the trace of the forward Mach cone in the  $z = 0$  plane

$[(x - x_o)^2 - \beta^2(y - y_o)^2 - \beta^2 z^2 = 0]$  and is therefore the appropriate root of the expression appearing in the denominator of the integrand. The roots are

$$y_a, y_b = \frac{-m(\beta^2 my - x) \pm \beta m \sqrt{(y - mx)^2 + (1 - \beta^2 m^2)z^2}}{(1 - \beta^2 m^2)} \quad (A1)$$

so that equation (11) may be rewritten

$$\frac{-2\pi(1 - \beta^2 m^2)^{\frac{3}{2}}}{\beta^2 m^2 \kappa (y - mx)} w = \sqrt{I} = \int_0^{y_b} \frac{dy_o}{[(y_a - y_o)(y_b - y_o)]^{3/2}} \quad (A2)$$

From equations (6) and (7),

$$\sqrt{I} = -J(0) - C \quad (A3)$$

where

$$J(0) = \frac{2(y_a + y_b)}{(y_a - y_b)^2 \sqrt{y_a y_b}}$$

and

$$\begin{aligned}
 C &= \lim_{y_o \rightarrow y_b} \left[ \frac{2A(y_b)}{\sqrt{y_b - y_o}} - J(y_o) \right] \\
 &= \lim_{y_o \rightarrow y_b} \left[ \frac{2}{(y_a - y_b)^{\frac{3}{2}} \sqrt{y_b - y_o}} - \frac{2(y_a + y_b - 2y_o)}{(y_a - y_b)^2 \sqrt{(y_a - y_o)(y_b - y_o)}} \right] \\
 &= 0
 \end{aligned}$$

Thus

$$\sqrt{I} = - \frac{2(y_a + y_b)}{(y_a - y_b)^2 \sqrt{y_a y_b}} \quad (A4)$$

Substituting equation (A4) in equation (A2) and solving for  $w$  yields

$$w = - \frac{\kappa}{2\pi} \frac{(y - mx)(\beta^2 m y - x)}{(x^2 - \beta^2 y^2 - \beta^2 z^2)^{\frac{1}{2}} \left[ (y - mx)^2 + (1 - \beta^2 m^2) z^2 \right]} \quad (A5)$$

## APPENDIX B

## LOADING IN VICINITY OF WING TIP

The nature of the loading in the vicinity of a wing tip formed by the intersection of a subsonic leading edge with a supersonic trailing edge (fig. 6) is to be determined.

According to linearized theory,  $u_T$  in the region of a subsonic leading edge is singular of the form

$$u_T = \frac{1}{\sqrt{x_0 - x_l}}$$

where  $x_l$  is the equation for the leading edge as a function of  $y_0$ . This relation may be deduced from equation (11) of reference 10. The corresponding wing circulation is

$$\Gamma = \Delta\varphi_t = 2 \int_{x_l}^{x_t} \frac{dx_0}{\sqrt{x_0 - x_l}} = 4 \sqrt{x_t - x_l} \quad (B1)$$

The derivative of equation (B1) is

$$\frac{d\Gamma}{dy_0} = \frac{2 \frac{d(x_t - x_l)}{dy_0}}{\sqrt{x_t - x_l}} \quad (B2)$$

where  $(x_t - x_l)$  is the wing chord as a function of  $y_0$ . However,  $(x_t - x_l)$  must be of the form

$$x_t - x_l = y_0 [f(y_0)] \quad (B3)$$

(where  $[f(y_0)] \neq 0, \infty$  in order to satisfy the restrictions  
 $y_0 = 0$   
 that at the wing tip

9 ETT  
(a) the chord is zero

$$(x_t - x_l)_{y_o=0} = 0$$

(b) the slopes of the leading and trailing edges are neither equal

$$\left[ \frac{d(x_t - x_l)}{dy_o} \right]_{y_o=0} \neq 0$$

nor in the free-stream direction

$$\left[ \frac{d(x_t - x_l)}{dy_o} \right]_{y_o=0} \neq \infty$$

Substituting equation (B3) into the denominator of equation (B2) yields

$$\frac{d\Gamma}{dy_o} = \frac{2 \frac{d(x_t - x_l)}{dy_o}}{\sqrt{y_o [f(y_o)]}} \quad (B4)$$

Equation (B4) indicates that  $d\Gamma/dy_o$  is singular of order 1/2 at  $y_o = 0$  for the wing tip of figure 6.

#### REFERENCES

1. Lagerstrom, P. A., and Graham, Martha E.: Downwash and Side-wash Induced by Three-Dimensional Lifting Wings in Supersonic Flow. Rep. No. SM-13007, Douglas Aircraft Co., Inc., April 1947.
2. Heaslet, Max A., and Lomax, Harvard: The Calculation of Downwash behind Supersonic Wings with an Application to Triangular Plan Forms. NACA TN 1620, 1948.

3. Lomax, Harvard, and Sluder, Loma: Downwash in the Vertical and Horizontal Planes of Symmetry behind a Triangular Wing. NACA TN 1803, 1949.
4. Robinson, A.: On Source and Vortex Distributions in the Linearized Theory of Steady Supersonic Flow. Rep. No. 9, College Aero. (Cranfield), Oct. 1947.
5. Robinson, A., and Hunter-Tod, J. H.: Bound and Trailing Vortices in the Linearized Theory of Supersonic Flow and the Downwash in the Wake of a Delta Wing. Rep. No. 10, College Aero. (Cranfield), Oct. 1947.
6. Hadamard, Jacques: Lectures on Cauchy's Problem in Linear Partial Differential Equations. Oxford Univ. Press (London), 1923, pp. 133-135.
7. Heaslet, Max A., and Lomax, Harvard: The Use of Source-Sink and Doublet Distributions Extended to the Solution of Arbitrary Boundary Value Problems in Supersonic Flow. NACA TN 1515, 1948.
8. Evvard, John C.: Distribution of Wave Drag and Lift in the Vicinity of Wing Tips at Supersonic Speeds. NACA TN 1382, 1947.
9. Evvard, John C.: Theoretical Distribution of Lift on Thin Wings at Supersonic Speeds (An Extension). NACA TN 1585, 1948.
10. Silverstein, Abe, Katzoff, S., and Bullivant, W. Kenneth: Downwash and Wake behind Plain and Flapped Airfoils. NACA Rep. 651, 1939.

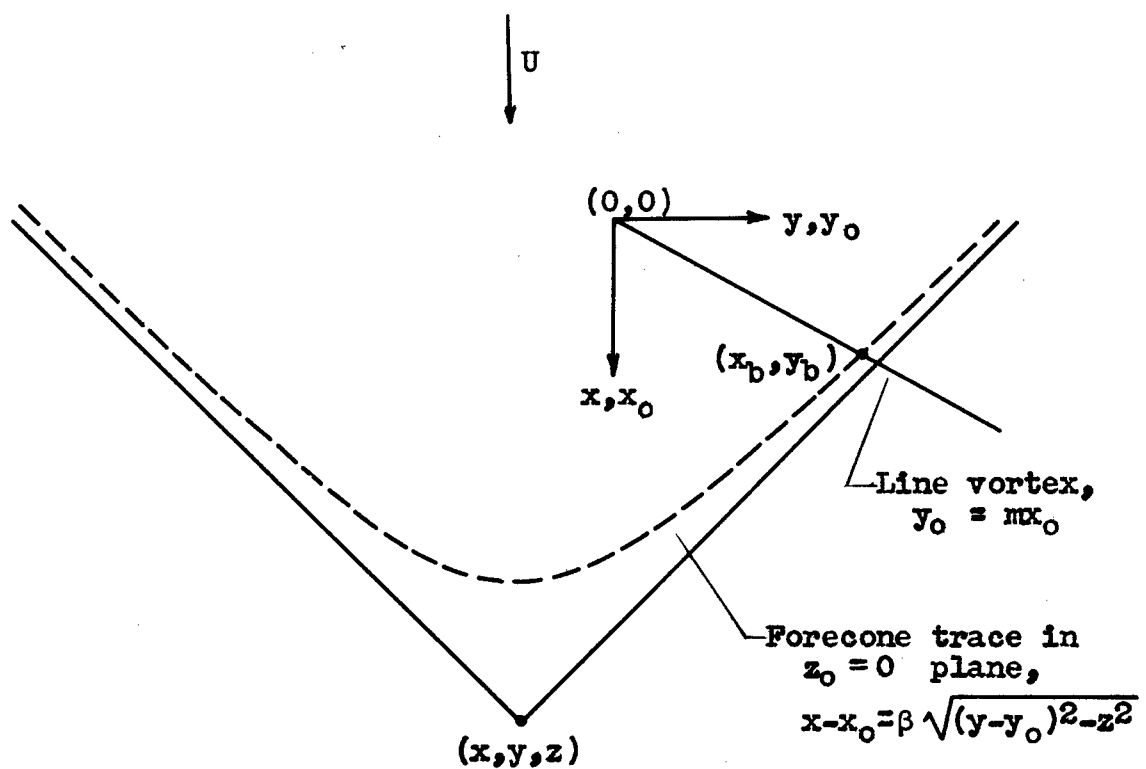


Figure 1. - Geometric relations for determination of upwash induced by line vortex.



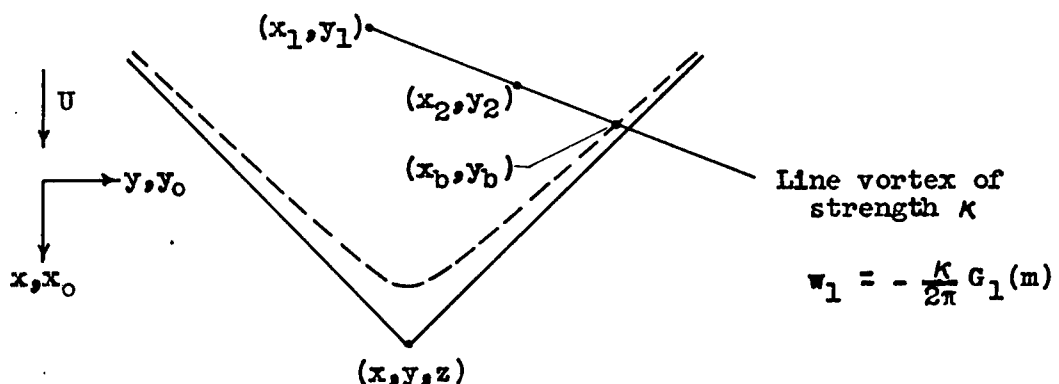
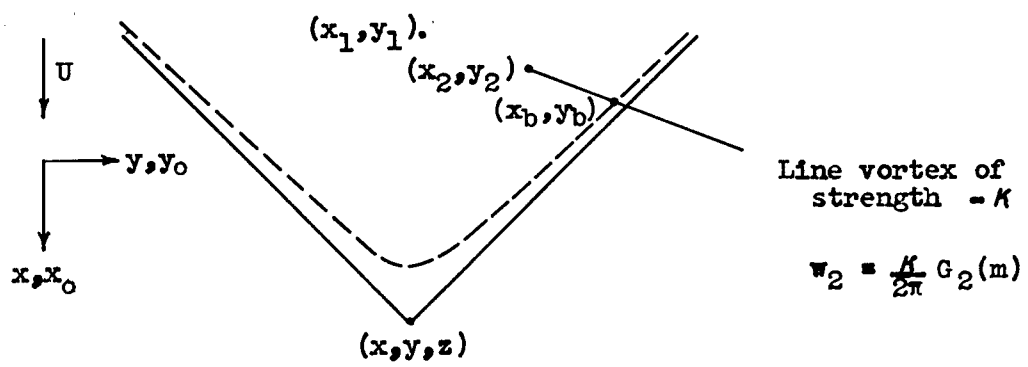
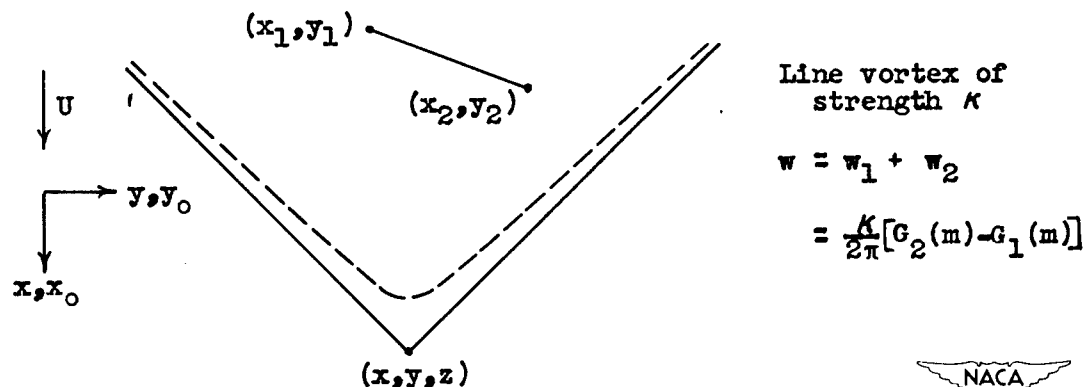
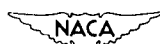
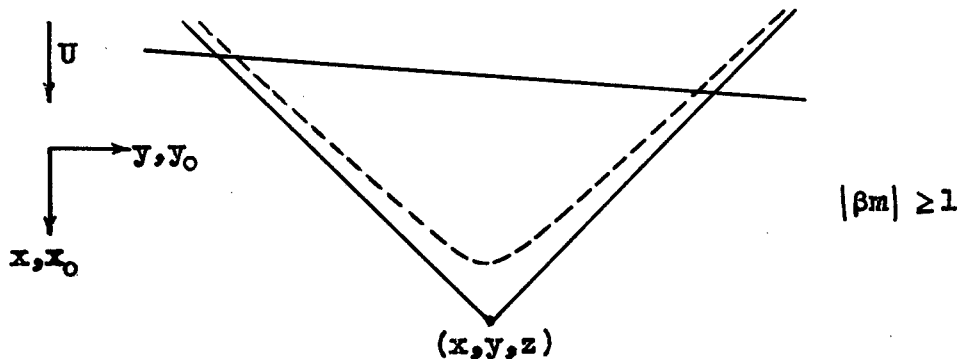
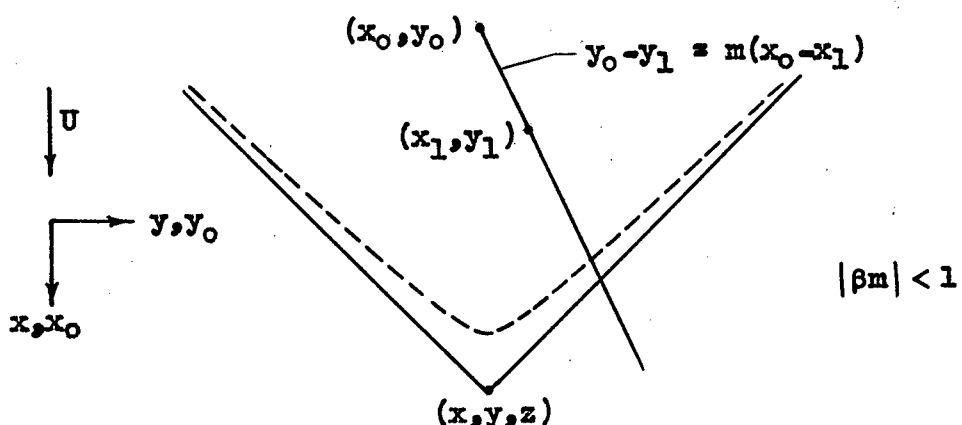
(a) Line vortex from  $(x_1, y_1)$ .(b) Line vortex from  $(x_2, y_2)$ .(c) Line vortex from  $(x_1, y_1)$  to  $(x_2, y_2)$ .

Figure 2. - Superposition for obtaining upwash induced by line-vortex segment from  $x_1, y_1$  to  $x_2, y_2$ .

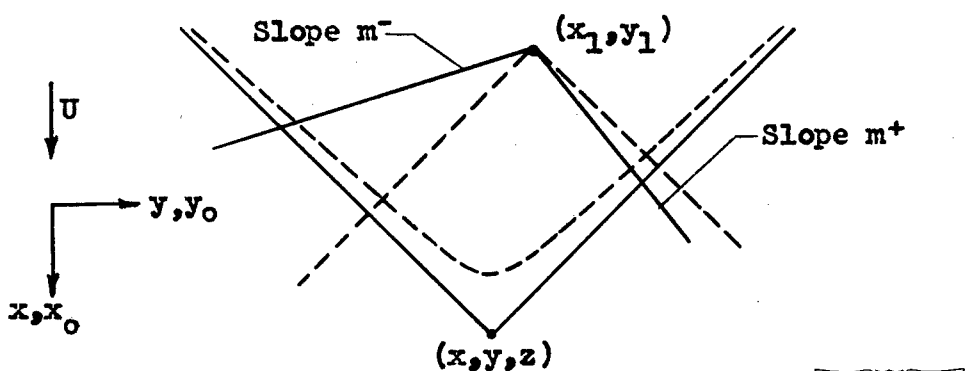




(a) Infinite line vortex inclined supersonically to free stream.



(b) Infinite line vortex inclined subsonically to free stream.



(c) Bent line vortex.



Figure 3. - Typical line vortices.

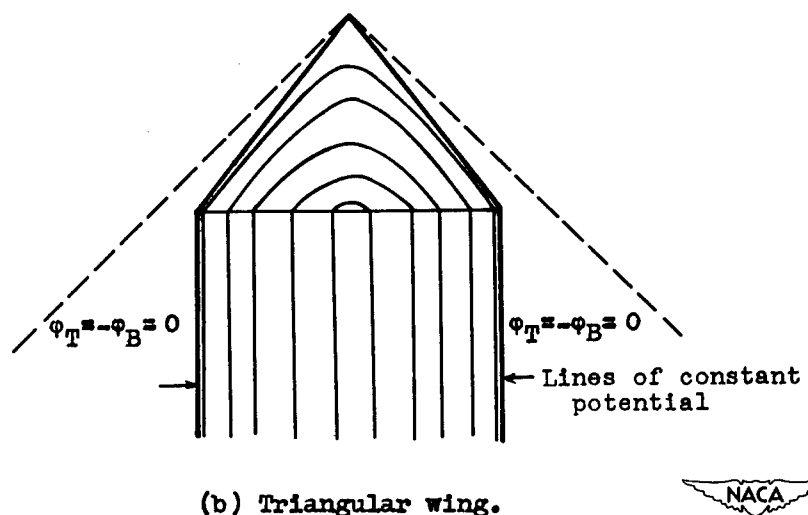
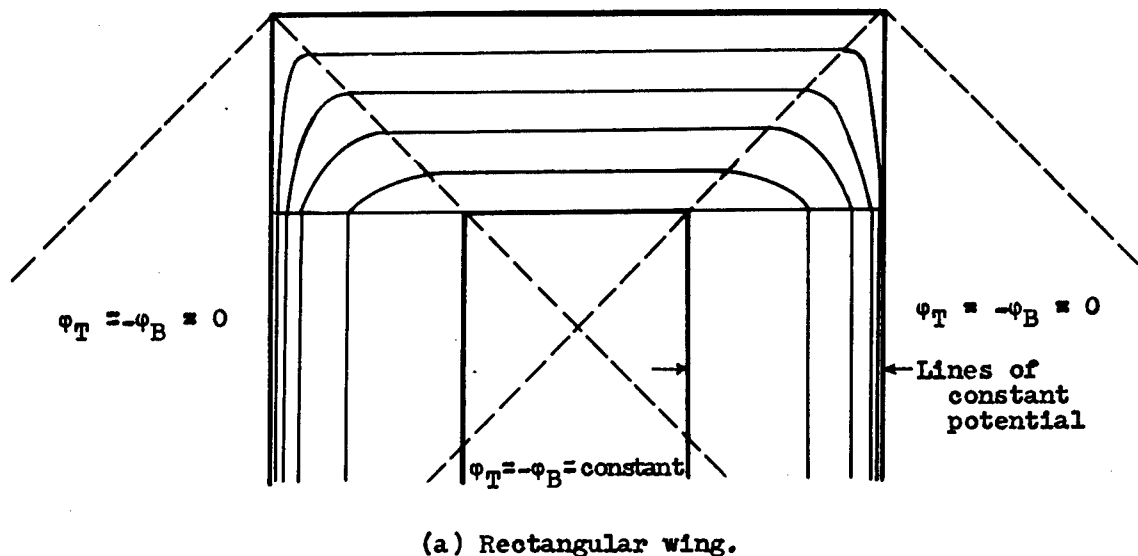
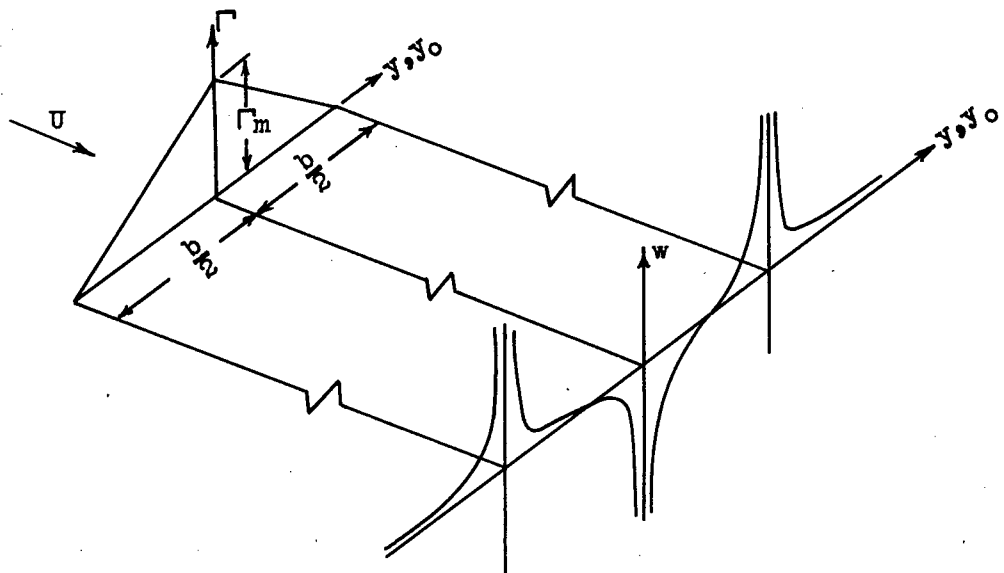
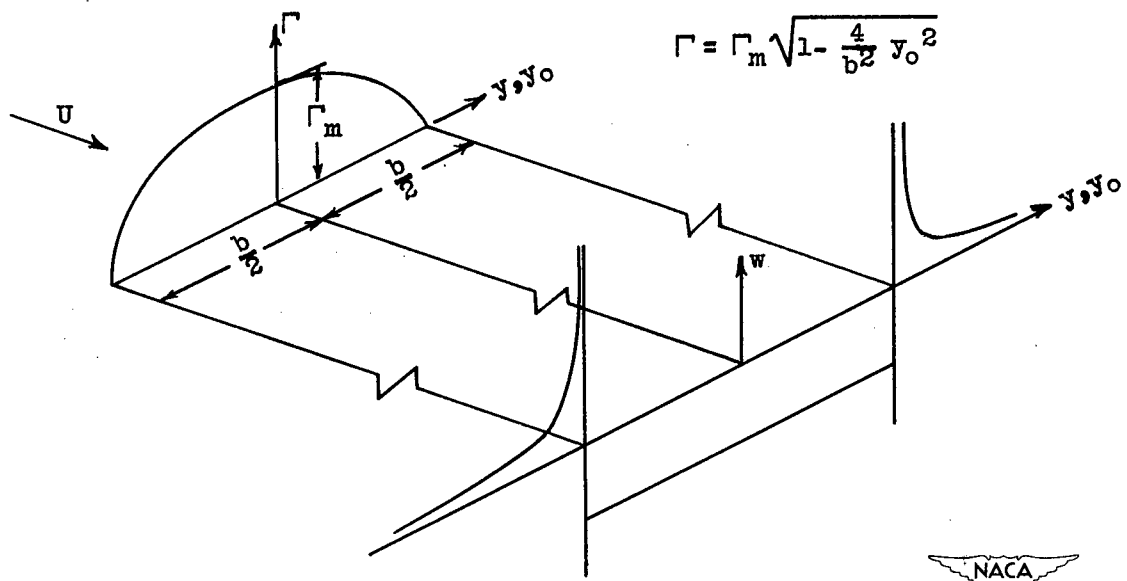


Figure 4. - Lines of constant potential for rectangular and triangular wings.

NACA



(a) Triangular load distribution.



(b) Elliptic load distribution.

Figure 5. - Upwash in  $z = 0$  plane an infinite distance behind wings of triangular and elliptic loading.

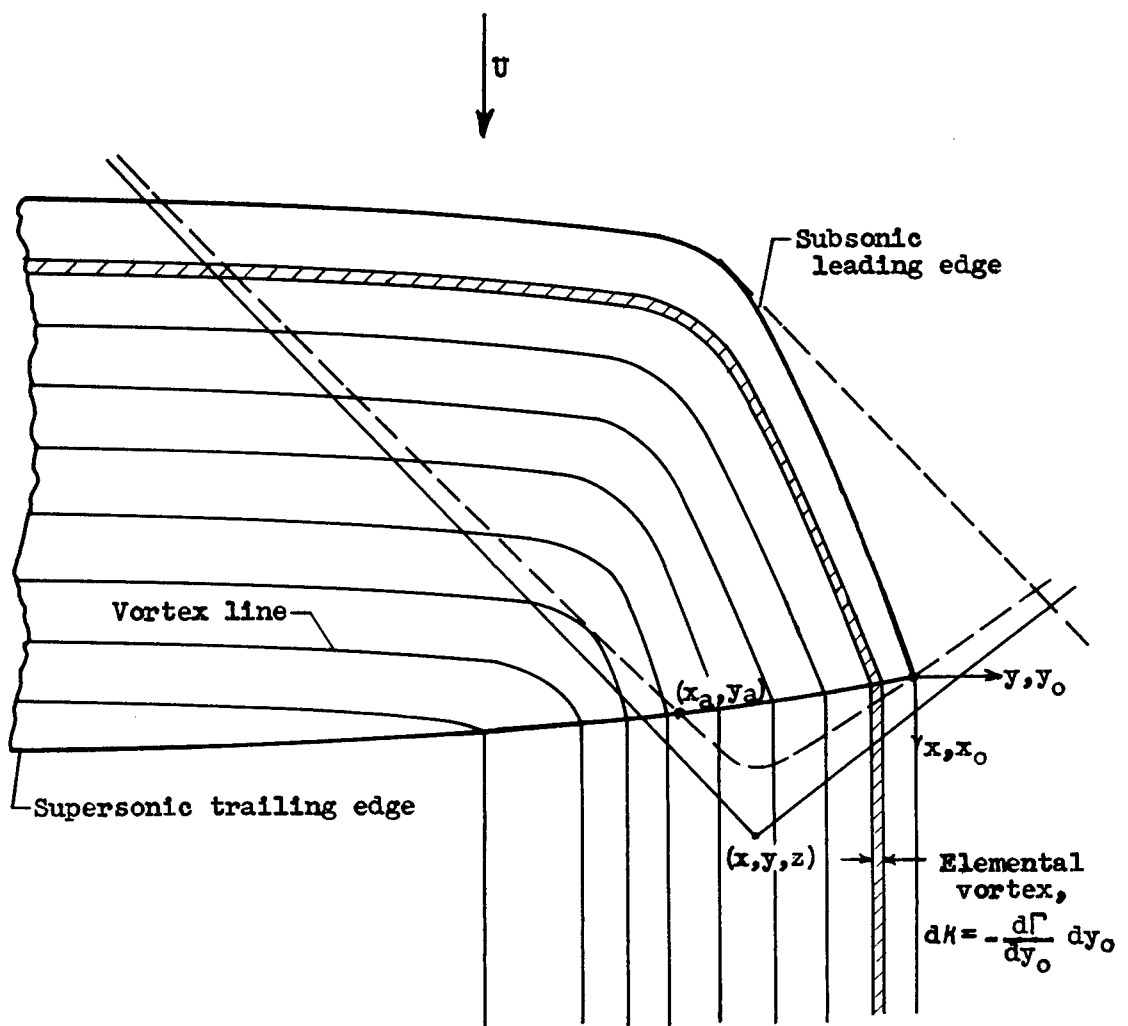


Figure 6. - Wing tip formed by intersection of subsonic leading and supersonic trailing plan-form edges.



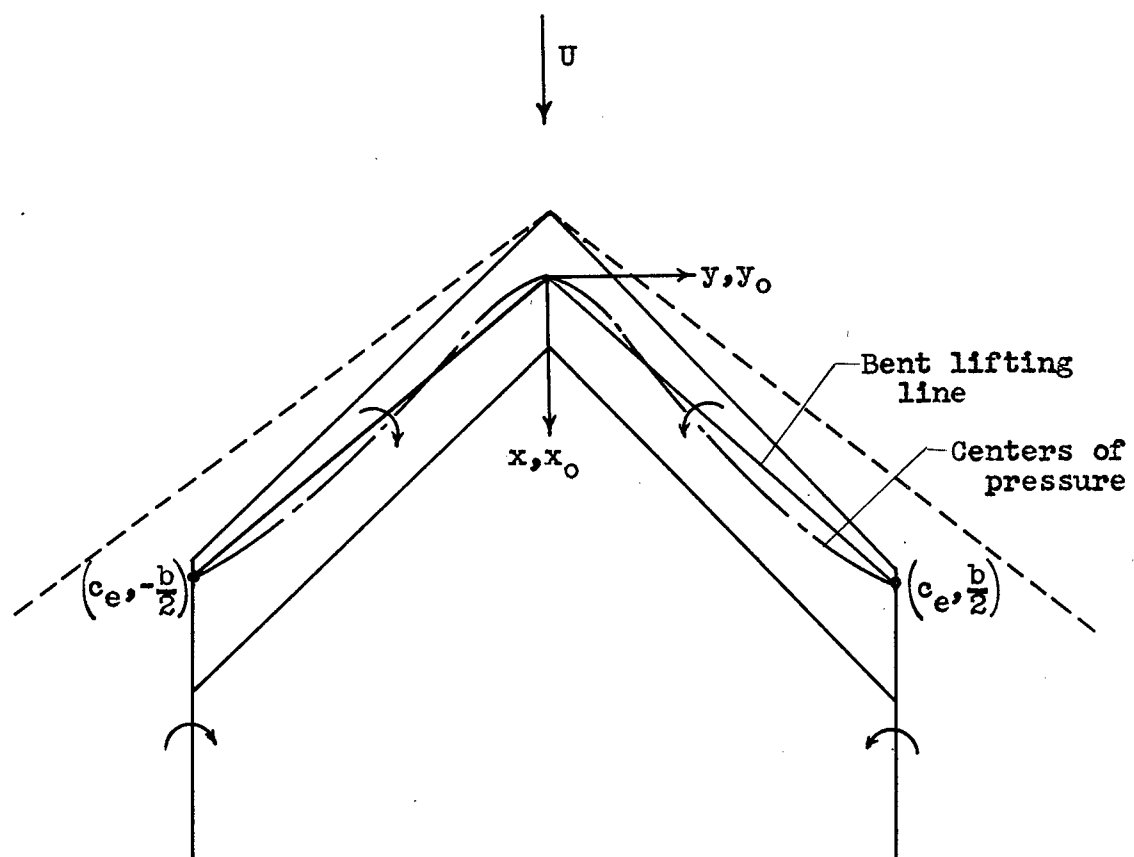
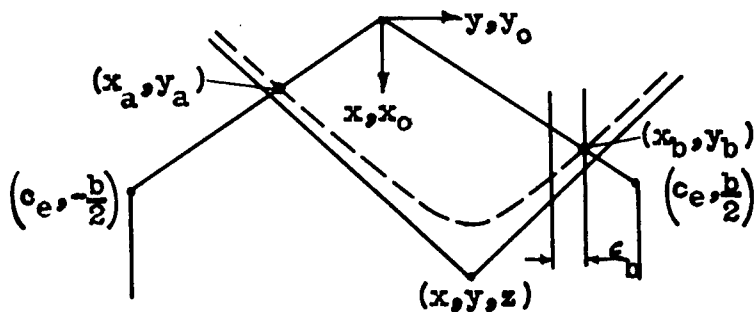
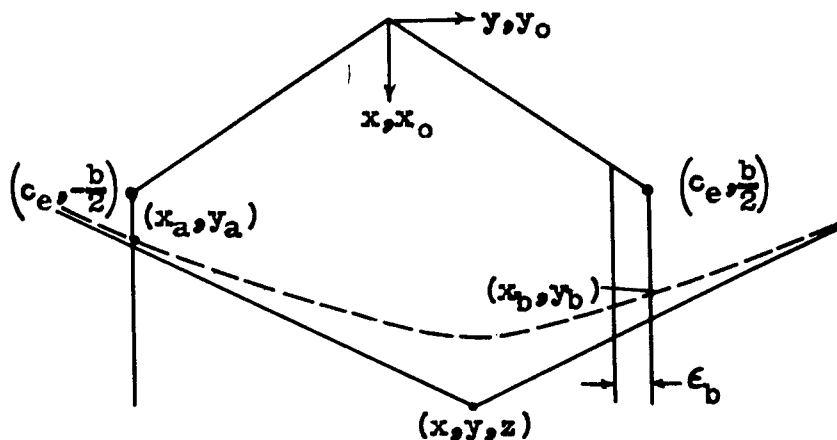


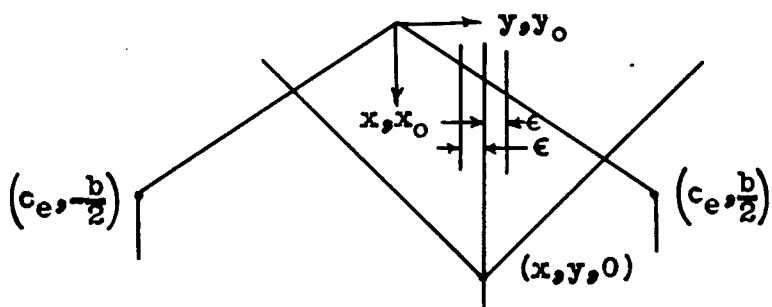
Figure 7. - Bent-lifting-line approximation for sweptback wing.



(a) Intersection of forecone with lifting line.



(b) Intersection of forecone with edge of vortex sheet.



(c) Point on vortex sheet.



Figure 8. - Improper intervals of downwash integral.

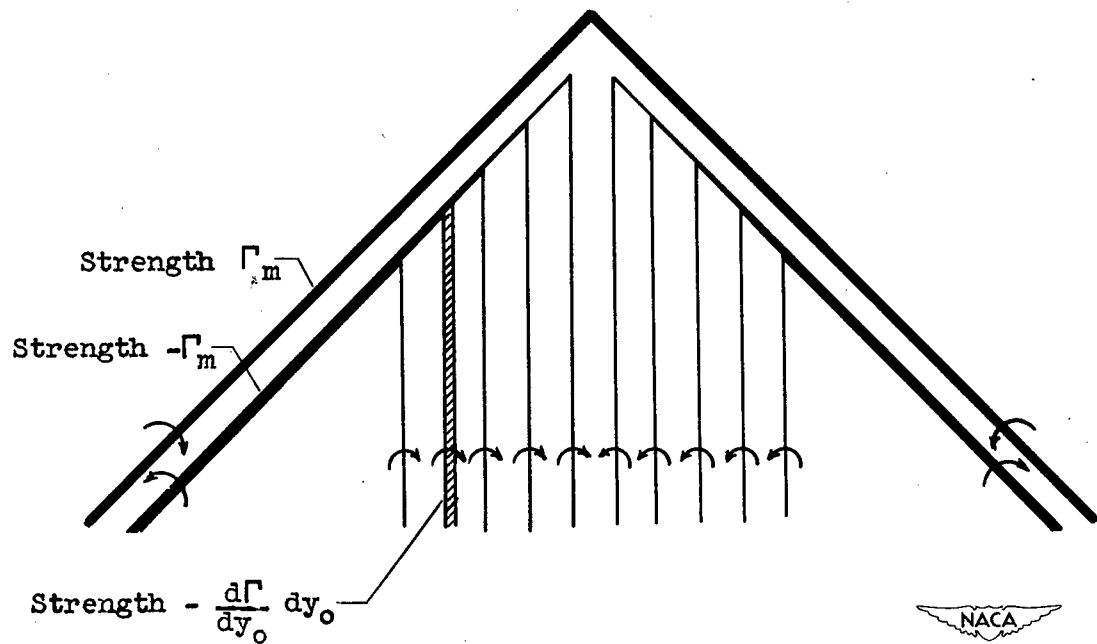
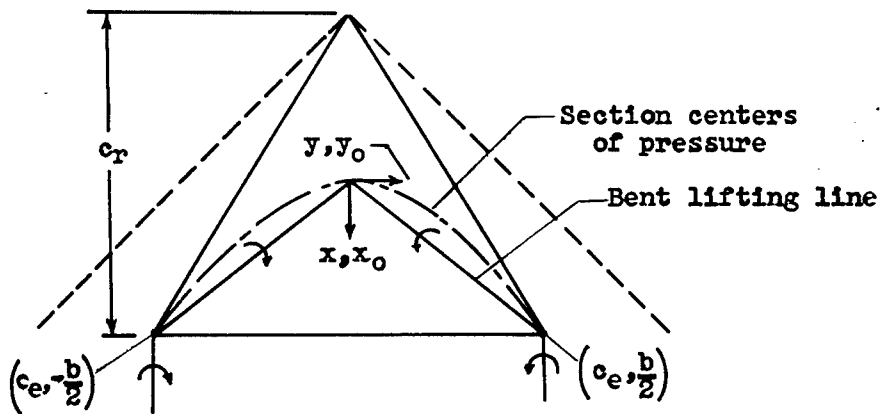
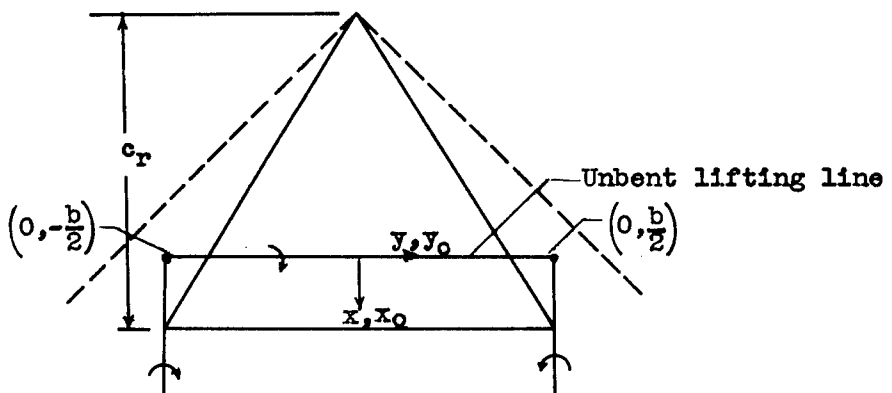


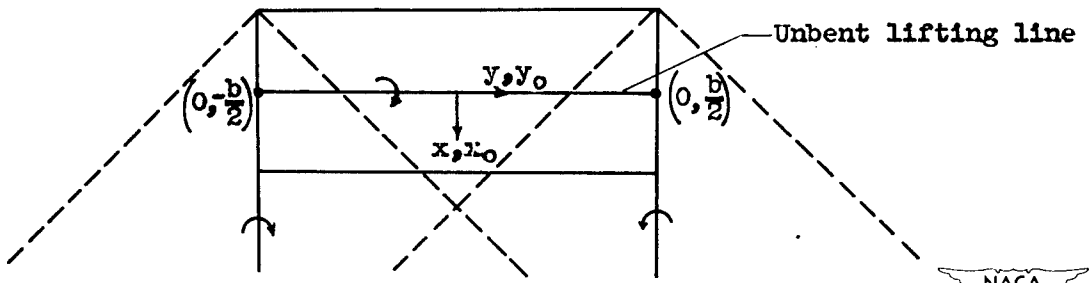
Figure 9. - Superposition of bent line vortices yielding bent-lifting-line representation of supersonic wing (equation (41)).



(a) Bent-lifting-line representation of triangular wing.



(b) Unbent-lifting-line representation of triangular wing.



(c) Unbent-lifting-line representation of rectangular wing.

Figure 10. - Lifting-line representations of triangular and rectangular wings.



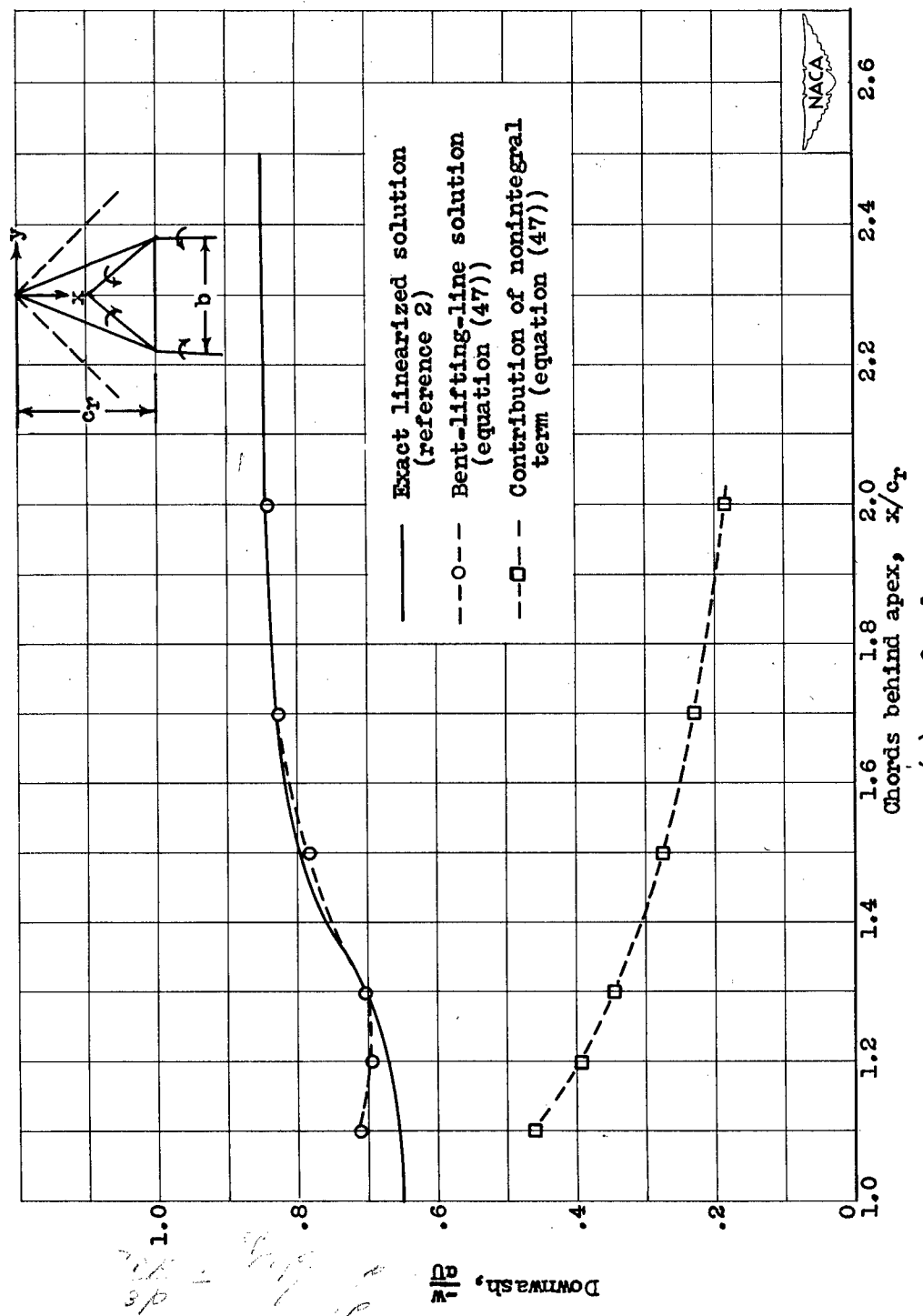


Figure 11. - Downwash in  $y=0$  plane behind triangular wing with aspect ratio  $\frac{2b}{c_r}$  of 1.6 using bent lifting line.  $M = \sqrt{2}$ .

(a)  $z = 0$  plane.

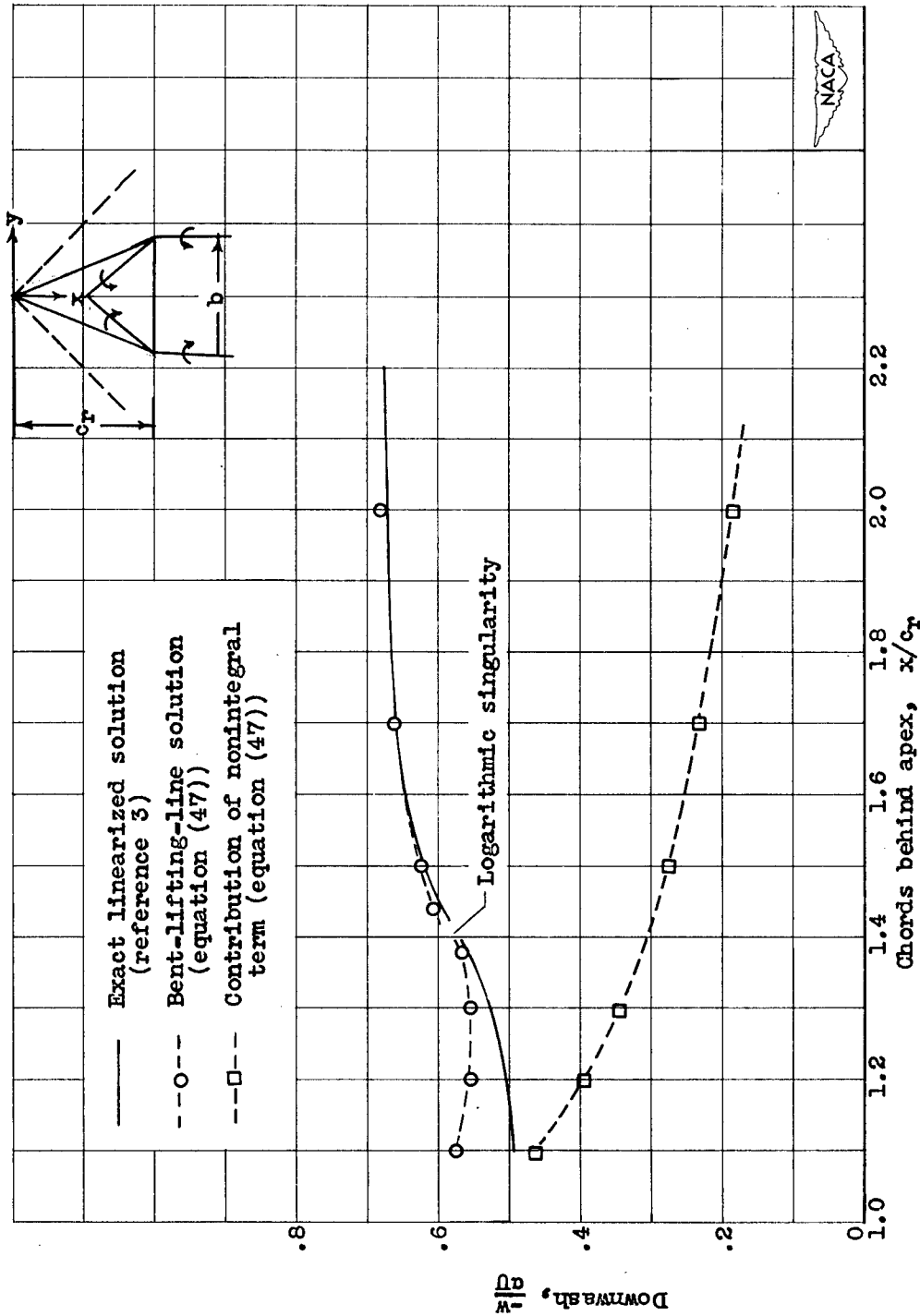


Figure 11. - Concluded. Downwash in  $y=0$  plane behind triangular wing with aspect ratio  $\frac{2b}{c_r}$  of 1.6 using bent lifting line.  $M = \sqrt{2}$ .

(b)  $z = 0.1 b$  plane.

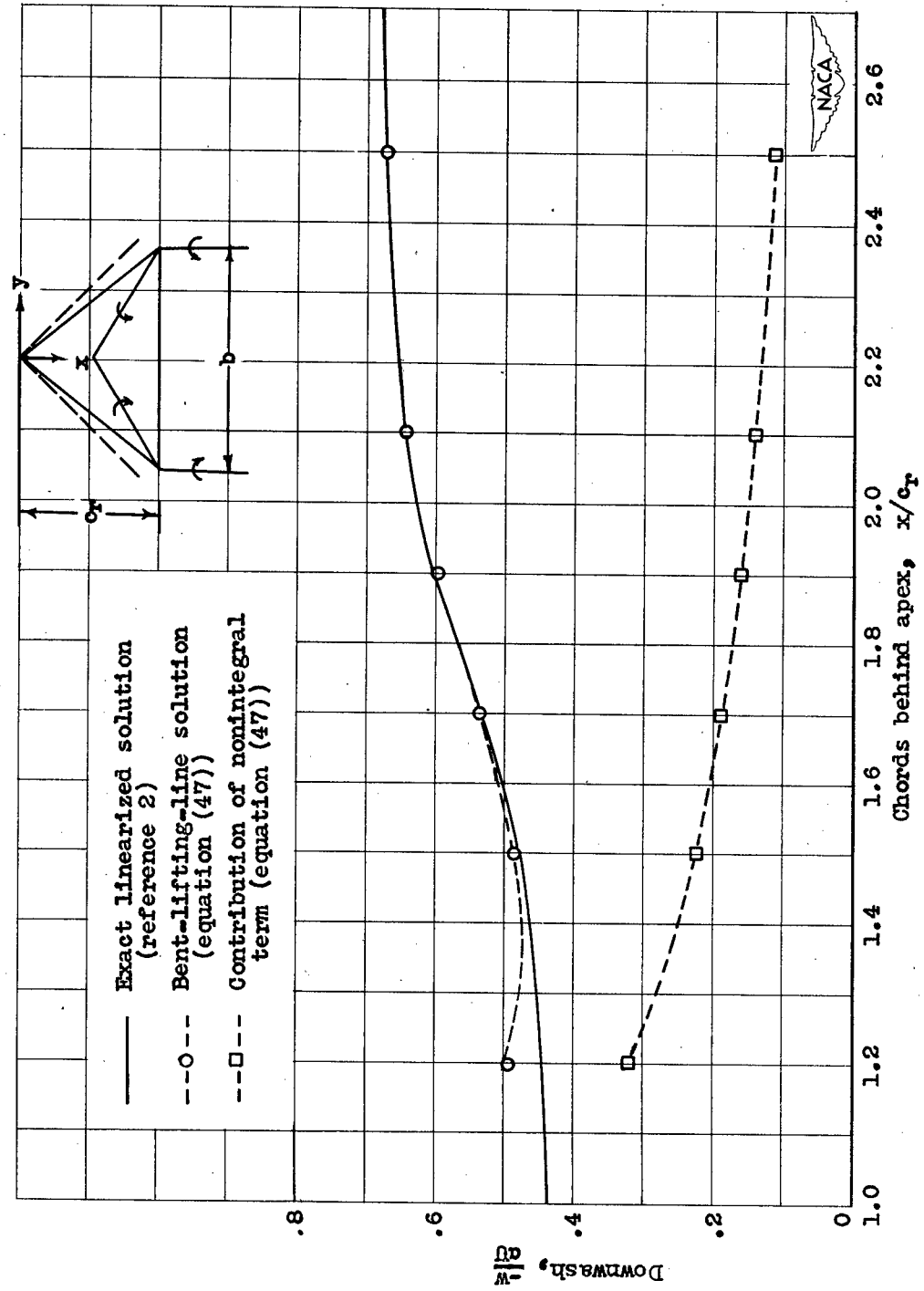


Figure 12. - Downwash in  $y=0$  plane behind triangular wing with aspect ratio  $2b/c_r$  of 3.2 using bent lifting line.  $M = \sqrt{2}$ .

① (a)  $z = 0$  plane.

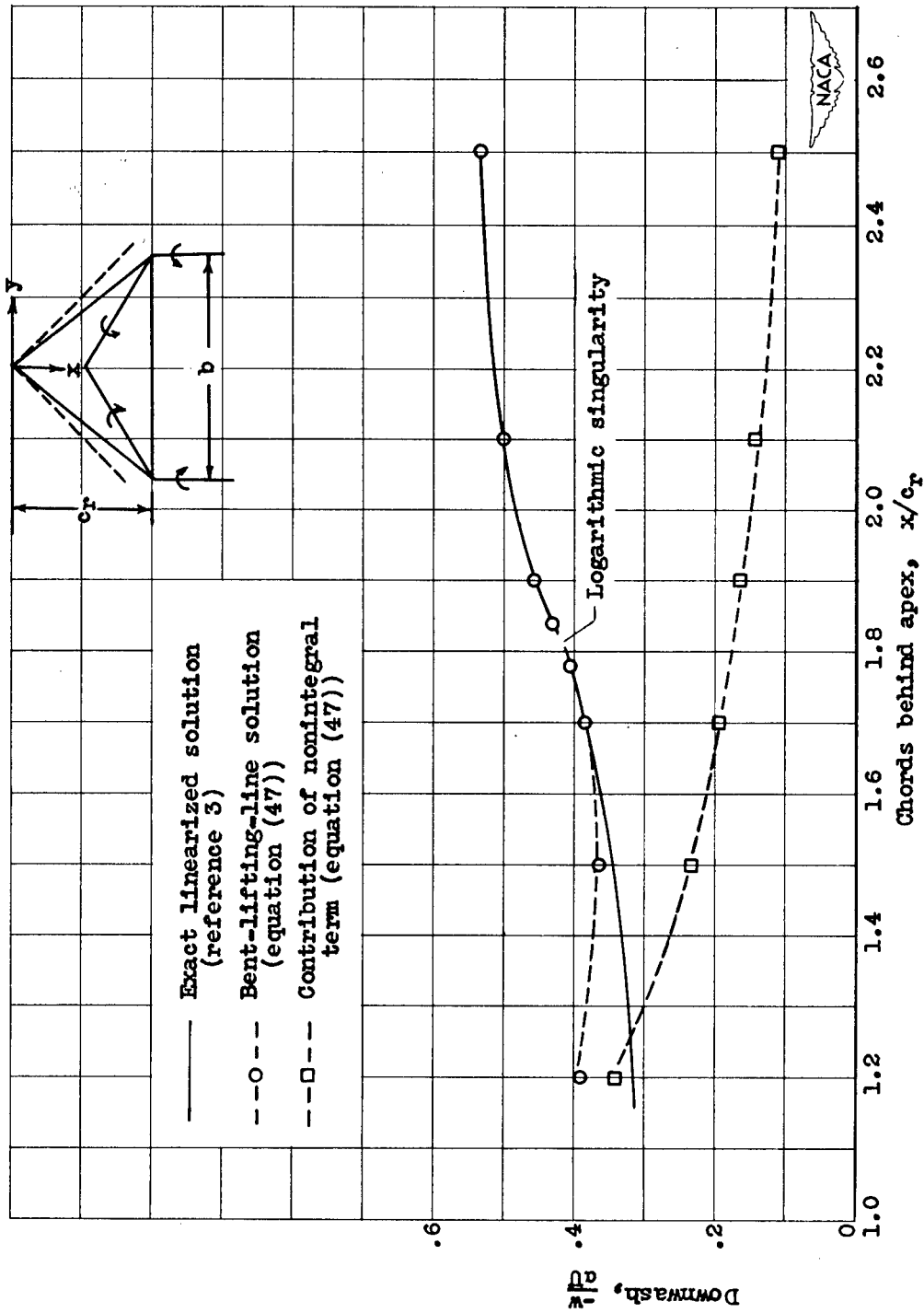


Figure 12. - Concluded. Downwash in  $y=0$  plane behind triangular wing with aspect ratio  $\frac{2b}{c_r}$  of 3.2 using bent lifting line.  $M = \sqrt{2}$ .

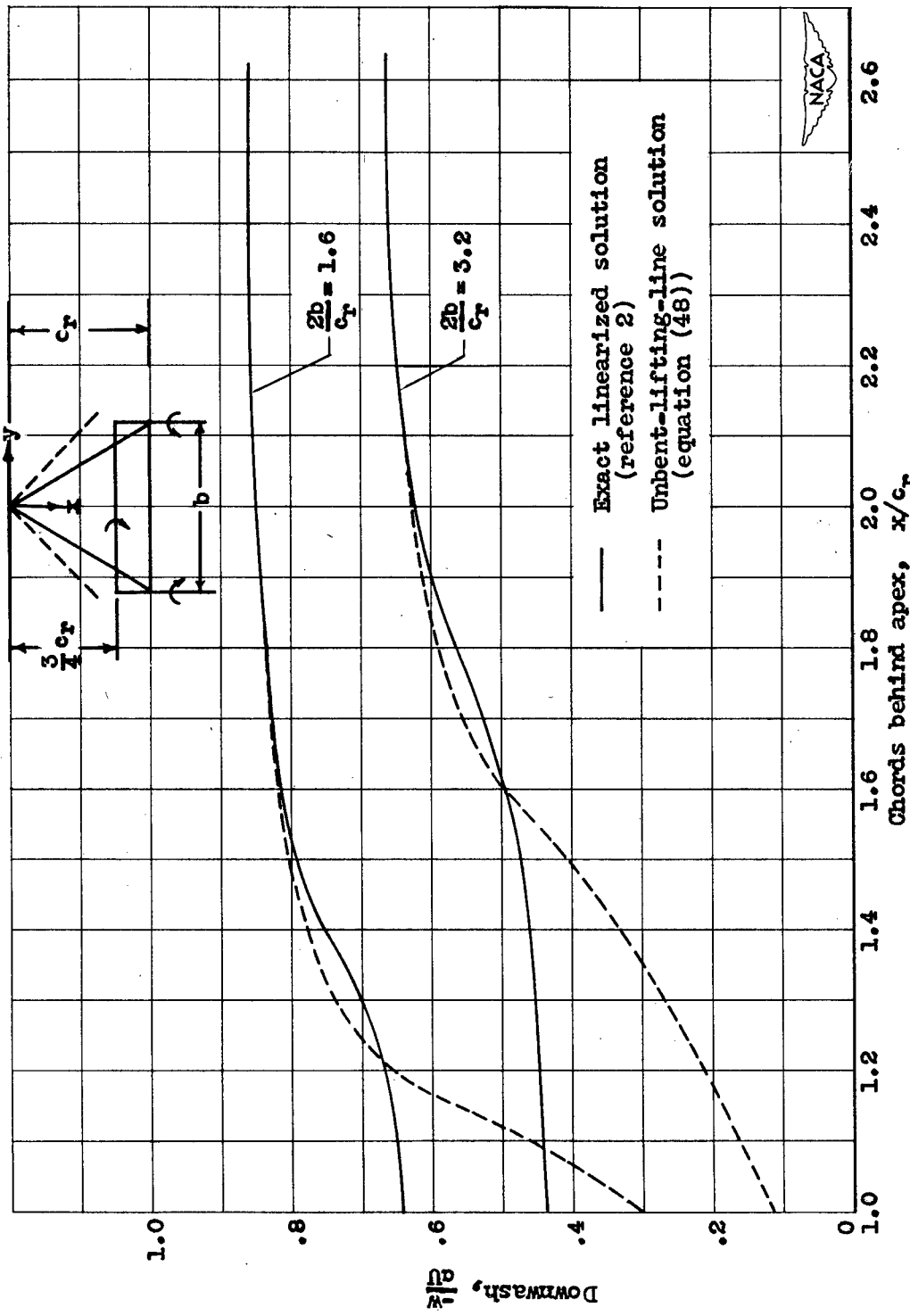


Figure 13. - Downwash along line  $y = 0$ ,  $z = 0$  behind triangular wing using unbent (horseshoe) lifting line at 3/4-chord point.  $M = \sqrt{2}$ .

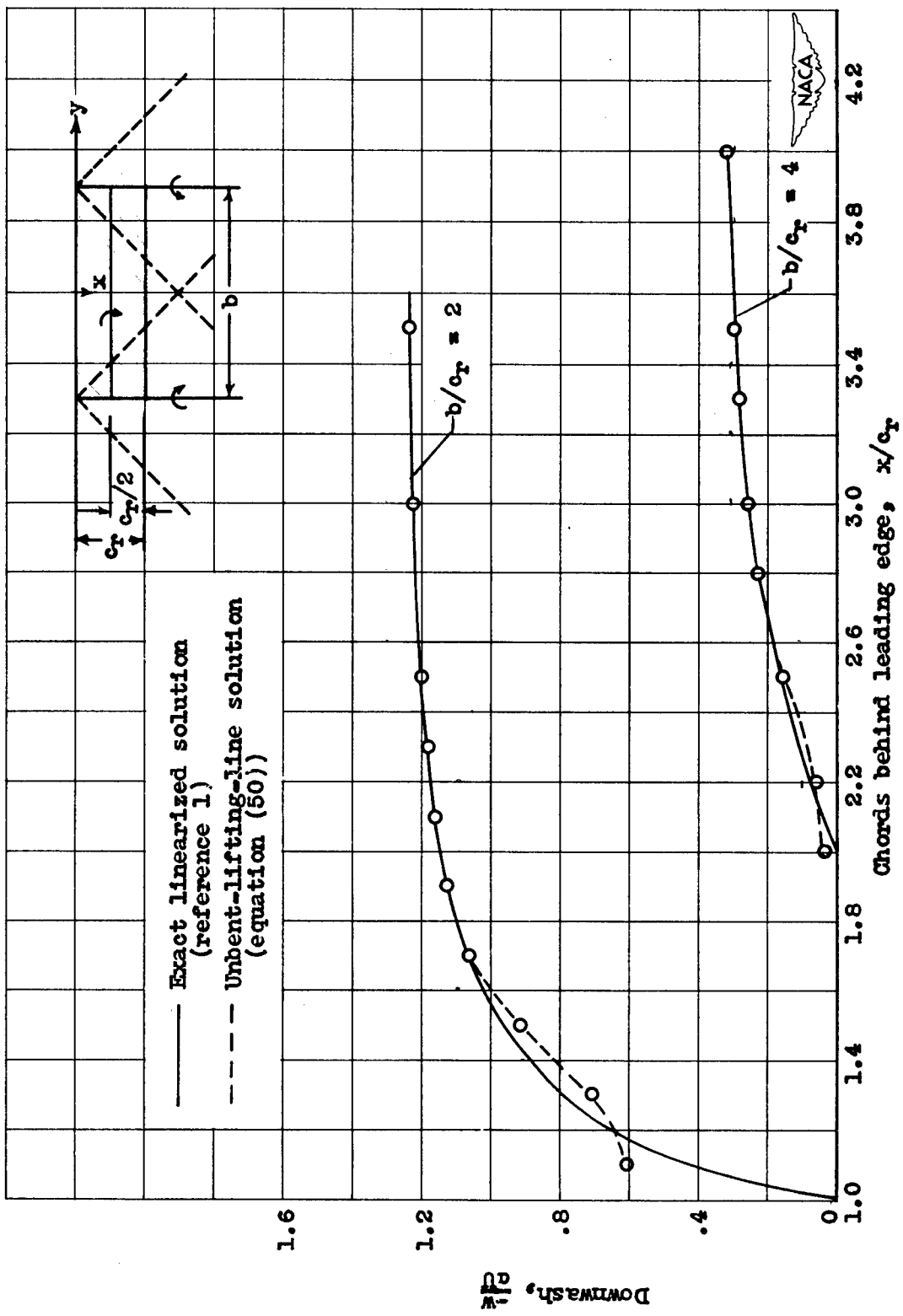


Figure 14. - Downwash along line  $y=0$ ,  $z=0$  behind rectangular wing using unbent (horseshoe) lifting line at 1/2-chord point.  $M = \sqrt{2}$ .